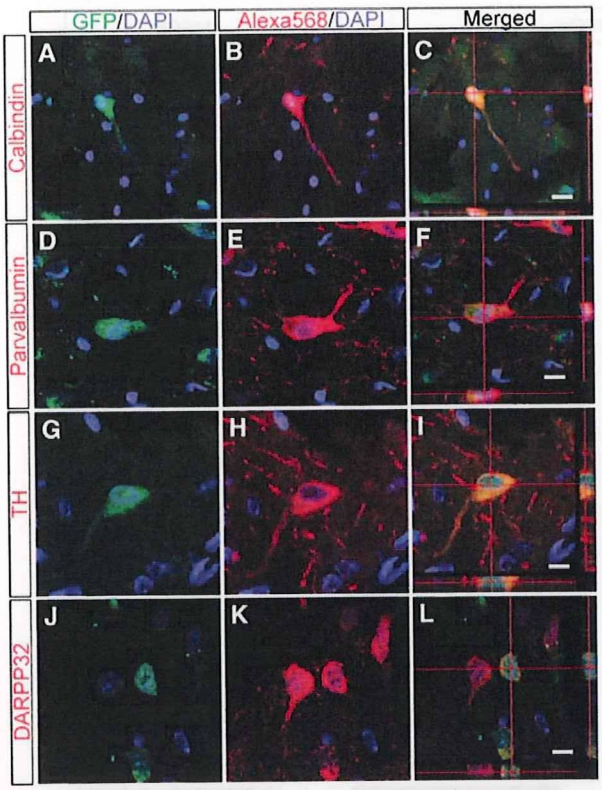

Figure 4 Immunohistochemistry of green fluorescent protein (GFP)-positive transplanted NS-MSCs (day 100). (**A–C**) Calbindin, (**D–F**) parvalbumin, (**G–I**) tyrosine hydroxylase (TH), (**J–L**) DARPP32. These cells are mostly observed in the lesion boundary. Scale bars = 20 μm.

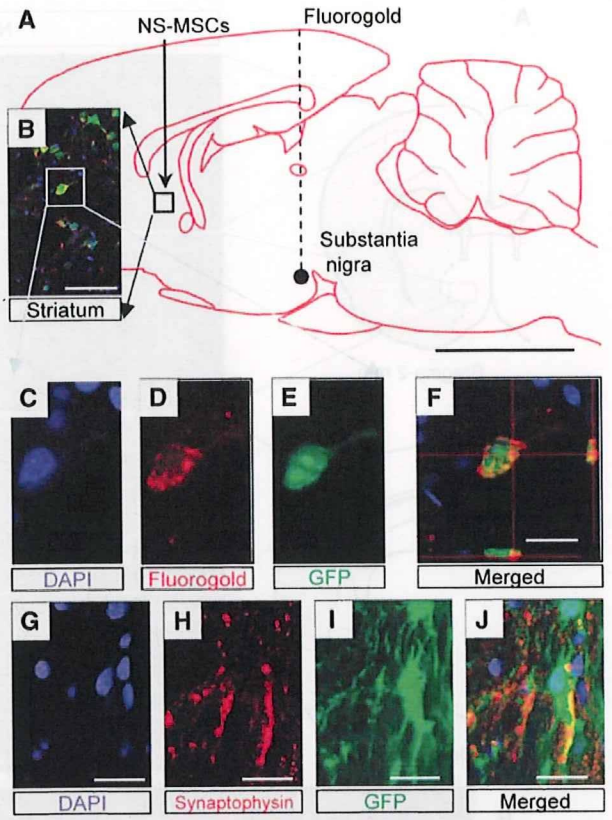

Figure 5 The expression of retrograde tracer Fluorogold injected in the targeted area of the substantia nigra and synaptophysin expression in the graft (day 100). (**A**) Site of NS-MSCs transplantation and Fluorogold injection. (**B**) Immunohistochemistry showed Fluorogold and green fluorescent protein (GFP) double-positive cells in the striatum. Higher magnification of 4′,6-diamidino-2-phenylindole (DAPI) (**C**), Fluorogold (**D**), and GFP (**E**) double-positive cells (**F**) with neuron-like morphology. (**G–J**) Synaptophysin is expressed in the perisynaptic areas of GFP-positive transplanted cells in the striatum. Scale bars = 5 mm (panel A), 100 μm (panel B), and 20 μm (panels C–J).

1% to 2%. The functional recovery induced by these naive MSCs transplantation may partly be mediated by the trophic effects of MSCs or by the intrinsic parenchymal cells stimulated by MSCs (Chen and Chopp, 2006; Li *et al*, 2002). However, in this study, a large number of GFP-labeled NS-MSCs was measured in the host brain even after 100 days of transplantation, and most of the cells expressed neuronal markers and neurotransmitter-related markers. In addition, Fluorogold tracing showed that the transplanted cells extended neurites for some distance in the host brain and might have formed synapses with host neurons. The true contribution of the neurite extension of transplanted NS-MSCs remains unclear; although our results suggest that the differentiation or orientation of MSCs into cells with neural properties before transplantation is effective for the survival and integration of MSCs.

In our result, recovery occurs long before the cells can have integrated into the host brain. In the limb-placing test, the MSC group showed slight recovery in the earlier period after operation, and the mean lesion volumes between the NS-MSCs and MSCs groups showed no statistical difference. Perhaps, the recovery in the earlier period (before 14 days) resulted from the trophic effect of transplanted cells rather than from the replenishment of lost cells. As mentioned above, naive MSCs are known to have trophic effects and therefore, it is no wonder that NS-MSCs also procure the same effect. However, in the later period, MSCs do not survive, whereas NS-MSCs do, which are migrated and differentiated in the host tissue. Although the cell replacement by transplanted NS-MSCs cannot be the entire contribution for the functional recovery, this difference may explain the functional recovery shown in NS-MSCs groups at a later period of 100 days.

Under stressful conditions, MSCs are shown to exhibit neuron-like morphology and to express neuronal markers, but without ever having undergone protein synthesis, indicating that the neuron-like morphologic and immunocytochemical changes are artifacts (Lu *et al*, 2004). Indeed, in their report,

NeuN and NSE were positive to these cells in immunocytochemistry, whereas upregulation of these markers could not be recognized in RT-PCR. In contrast, we confirmed the clear upregulation of NSE after neuronal induction from NS-MSCs, and expression of ChAT, one of the markers for functional neurons, in RT-PCR (Supplementary Figure 1). In real-time PCR, both NSE and voltage-gated sodium channel type III Scn3a were shown to be expressed substantially in neuronal cells induced from NS-MSCs but not in naive MSCs (Supplementary Figure 2). High performance liquid chromatograph also showed the effective production of dopamine from neuronal cells induced from NS-MSCs. These results collectively suggest that, different from stress-induced neuron-like cells, neuronal cells differentiated from NS-MSCs are functional as the upregulation of markers related to functional neurons are shown as described above.

Compared with fully differentiated postmitotic neuronal cells, NS-MSCs have several advantages. First, because of the premature state of NS-MSCs, they have a greater survival rate, distribution, and integration in the host brain. For differentiated dopaminergic neurons induced from MSCs (Dezawa *et al*, 2004; Mimura *et al*, 2005), the survival ratio was only 20% to 30% after transplantation into the Parkinson's disease model rat and their distribution was mostly confined to the striatum, suggesting their limited ability for migration and integration in the host tissue. However, NS-MSCs were widely observed in the lesion boundary, ipsilateral cortex, and striatum in the stroke brain and $21 \pm 1.3 \times 10^4$ cells were counted after the transplantation of 50,000 cells. As 4.7% of GFP-positive NS-MSCs were positive for Ki67 at 14 days, but GFP-positive cells were negative for Ki67 at 100 days, a subpopulation of NS-MSCs might have proliferated at an earlier period, but most of them became postmitotic by day 100. These observations might partly explain the following: (1) the ability of NS-MSCs to proliferate and migrate because of their premature state and (2) although NS-MSCs show neural lineage commitment *in vitro*, their differentiation into functional neuronal subtypes in the host tissue, such as dopaminergic, glutamatergic, and GABAergic marker-positive cells might subsequently be regulated by the host microenvironment.

Second, NS-MSCs differentiated into various kinds of transmitter-related marker positive cells within the host brain. They also extended neurites for a long distance for ~ 6.3 mm. This suggests that premature NS-MSCs have higher flexibility to adapt to the host microenvironment and to differentiate into various cell types rather than fully differentiated neuronal cells. Such properties would be beneficial when replenishing neural cells are required to cover a large degenerated region and various types of neural cells are required, such as in the case of stroke. Conversely, in Parkinson's disease, as dopamine-producing cells are the main target, induction and differentiation into dopaminergic neurons before the transplantation would be preferable for functional recovery (Dezawa *et al*, 2004; Mimura *et al*, 2005).

Third, NS-MSCs are more easily prepared than fully differentiated neuronal cells, which might be beneficial from a practical aspect. Precise control and maintenance are required to achieve the differentiation of neuronal cells from human MSCs, appropriate density in the case of seeding and pertinent harvesting method. As for the NS-MSCs method, this free-floating culture method is not highly dependent on cell density and does not require harvesting. Moreover, in general, mature neurons are vulnerable compared with neural progenitors for their maintenance. Considering these three aspects, the NS-MSCs method will clinically be feasible for treating acute injuries like stroke.

Earlier reports have described the induction of neurosphere-like cells from MSCs using trophic factors and/or the medium used for neural stem cells (Hermann *et al*, 2004; Lee *et al*, 2003). Notably, in these reports, the ratio of glial cell differentiation is higher than that of neuronal cells; induction rates of mature neurons versus astrocytes derived from neurosphere-like cells are $6 \pm 2\%$:$13 \pm 4\%$ (Hermann *et al*, 2004) or 6.5%:32.9% (Lee *et al*, 2003). In our system, almost all of the NS-MSCs differentiated into neuronal cells and a very small number of glial cells were produced, both *in vitro* and *in vivo*. This finding suggests that NICD introduction and sphere formation strongly shifted the MSCs to a neuronal potential.

The number of GFP-labeled transplanted cells at 100 days after transplantation was four times higher than that at 14 days. Therefore, we conducted the study on Ki67 staining, a marker for cell proliferation related to tumor genesis, which showed that Ki67-positive cells were detected in 14 but not in 100 days. Furthermore, the percentage of GFP-positive cells that expressed NeuN at 100 days was very high ($79.5 \pm 0.1\%$). Some of them might get disposed from the organism after transplantation, but overall, this result suggests that large number of Ki67-positive cells at 14 days did not continue to divide and differentiated into neuronal phenotype by 100 days. Consistently, the ability to generate spheres was limited in NS-MSCs, i.e., NS-MSCs could generate second and third spheres but were unable to show fourth sphere formation. In addition, tumor formation was not detected up to 100 days. Many reports suggested that MSCs are less tumorigenic than fetus-derived stem cells or embryonic stem cells, and few reports with regard to MSC transplantation into stroke model animals reported ectopic tissue formation or carcinogenesis (Chen *et al*, 2001*a*, *b*). Indeed, these earlier reports do not completely cast aside the tumorigenic possibility of MSC or MSC-derived cells. The most reliable safety evaluation will not be performed in the rat experiment but in the higher mammals like monkeys; therefore, we recognize that

evaluation in the monkey experiment is necessary in the future.

Notch signaling inhibits neuronal differentiation and promotes glial differentiation during development (Lundkvist and Lendahl, 2001). Although our results seem inconsistent with the well-known action of Notch signaling, it is presumed that cell susceptibility to Notch signaling in MSCs is different from cells in the process of neuronal development. Our results suggest distinct cellular responses to Notch signals; e.g., the protein repertoire and active factors may be quite different between conventional neural progenitor cells and MSCs. We recognized in this experiment that NICD transfection leads to an upregulation of NeuroD in the luciferase assay as described earlier (Dezawa *et al*, 2004), which suggests that, at least in MSCs, cells are orientated to a neural differentiation by NICD introduction. Furthermore, treatment with the free-floating culture system might have selected cells with a high potential for neural differentiation. The precise mechanism underlying the MSCs acquisition of neural progenitor cell properties in this system needs to be clarified.

Several reports indicated that remote degeneration of neurons together with the change in *Bcl-2* and tumor necrosis factor-α expression level occurs in the substantia nigra after focal ischemia (Arango-Davila *et al*, 2004; Loos *et al*, 2003). These observations suggested that the nigrostriatal pathway was damaged after focal ischemia. Earlier reports showed the improvement of behavioral dysfunction after striatal transplantation of embryonic stem cells, which was assessed by methamphetamine injection, the test known to estimate the nigrostriatal pathway (Yanagisawa *et al*, 2006). The result indicated that striatal transplantation could repair the damage of the nigrostriatal pathway. Our result also showed the same effect of striatal transplantation.

Furthermore, several earlier studies indicated that hemispheric damage influenced the result of water-maze test (Puurunen *et al*, 2001; Veizovic *et al*, 2001). In addition, Yonemori *et al* (Yonemori *et al*, 1999) reported that focal cerebral ischemia caused spatial memory disturbance in rats. Therefore, in our experiment, the improvement of this test might have been brought about by the improvement of both cognitive and motor functions.

Human MSCs have a high proliferation ability; 20 to 100 mL of bone marrow aspirate provides 1×10^7 MSCs within several weeks. Considering the sphere formation efficiency described above, as many as 5×10^4 spheres may be obtained from a patient's bone marrow within a reasonable time period. We also confirmed that cryopreserved NS-MSCs could proliferate and repeatedly form spheres while maintaining their neural progenitor-like characteristics (data not shown). Therefore, not only for autologous transplantation, but also for a cell-providing system using the same human leukocyte antigen subtype, MSCs from a healthy donor might be a realistic approach for cell therapy. This MSC cell therapy approach may be applicable for stroke victims and for those of other neurodegenerative diseases.

Acknowledgements

We thank Dr M Bohn (Northwestern University, Chicago) for giving us helpful advice and for editing our paper.

Conflict of interest

The authors declare no conflict of interest.

References

Abercrombie M (1946) Estimation of nuclear population from microtome sections. *Anat Rec* 94:239–47

Arango-Davila CA, Cardona-Gomez GP, Gallego-Gomez JC, Garcia-Segura LM, Pimienta HJ (2004) Down-regulation of Bcl-2 in rat substantia nigra after focal cerebral ischemia. *Neuroreport* 15:1437–41

Bliss T, Guzman R, Daadi M, Steinberg GK (2007) Cell transplantation therapy for stroke. *Stroke* 38:817–26

Borlongan CV, Hadman M, Sanberg CD, Sanberg PR (2004) Central nervous system entry of peripherally injected umbilical cord blood cells is not required for neuroprotection in stroke. *Stroke* 35:2385–9

Chen J, Chopp M (2006) Neurorestorative treatment of stroke: cell and pharmacological approaches. *NeuroRx* 3:466–73

Chen J, Li Y, Wang L, Lu M, Zhang X, Chopp M (2001*a*) Therapeutic benefit of intracerebral transplantation of bone marrow stromal cells after cerebral ischemia in rats. *J Neurol Sci* 189:49–57

Chen J, Sanberg PR, Li Y, Wang L, Lu M, Willing AE, Sanchez-Ramos J, Chopp M (2001*b*) Intravenous administration of human umbilical cord blood reduces behavioral deficits after stroke in rats. *Stroke* 32:2682–8

De Ryck M, Van Reempts J, Borgers M, Wauquier A, Janssen PA (1989) Photochemical stroke model: flunarizine prevents sensorimotor deficits after neocortical infarcts in rats. *Stroke* 20:1383–90

Dezawa M, Hoshino M, Nabeshima Y, Ide C (2005) Marrow stromal cells: implications in health and disease in the nervous system. *Curr Mol Med* 5:723–32

Dezawa M, Kanno H, Hoshino M, Cho H, Matsumoto N, Itokazu Y, Tajima N, Yamada H, Sawada H, Ishikawa H, Mimura T, Kitada M, Suzuki Y, Ide C (2004) Specific induction of neuronal cells from bone marrow stromal cells and application for autologous transplantation. *J Clin Invest* 113:1701–10

Dezawa M, Takahashi I, Esaki M, Takano M, Sawada H (2001) Sciatic nerve regeneration in rats induced by transplantation of in vitro differentiated bone-marrow stromal cells. *Eur J Neurosci* 14:1771–6

Hayashi J, Takagi Y, Fukuda H, Imazato T, Nishimura M, Fujimoto M, Takahashi J, Hashimoto N, Nozaki K (2006) Primate embryonic stem cell-derived neuronal progenitors transplanted into ischemic brain. *J Cereb Blood Flow Metab* 26:906–14

Hermann A, Gastl R, Liebau S, Popa MO, Fiedler J, Boehm BO, Maisel M, Lerche H, Schwarz J, Brenner R, Storch A (2004) Efficient generation of neural stem cell-like cells from adult human bone marrow stromal cells. *J Cell Sci* 117:4411–22

Igura K, Zhang X, Takahashi K, Mitsuru A, Yamaguchi S, Takashi TA (2004) Isolation and characterization of mesenchymal progenitor cells from chorionic villi of human placenta. *Cytotherapy* 6:543–53

In 't Anker PS, Scherjon SA, Kleijburg-van der Keur C, Noort WA, Claas FH, Willemze R, Fibbe WE, Kanhai HH (2003) Amniotic fluid as a novel source of mesenchymal stem cells for therapeutic transplantation. *Blood* 102:1548–9

Jeong SW, Chu K, Jung KH, Kim SU, Kim M, Roh JK (2003) Human neural stem cell transplantation promotes functional recovery in rats with experimental intracerebral hemorrhage. *Stroke* 34:2258–63

Koizumi J (1986) Experimental studies of ischemic brain edema: 1. A new experimental model of cerebral embolism in rats in which recirculation can be introduced in the ischemic area. *Jpn J Stroke* 8:1–8

Lee J, Elkahloun AG, Messina SA, Ferrari N, Xi D, Smith CL, Cooper Jr R, Albert PS, Fine HA (2003) Cellular and genetic characterization of human adult bone marrow-derived neural stem-like cells: a potential antiglioma cellular vector. *Cancer Res* 63:8877–89

Li Y, Chen J, Chen XG, Wang L, Gautam SC, Xu YX, Katakowski M, Zhang LJ, Lu M, Janakiraman N, Chopp M (2002) Human marrow stromal cell therapy for stroke in rat: neurotrophins and functional recovery. *Neurology* 59:514–23

Li Y, Chopp M, Chen J, Wang L, Gautam SC, Xu YX, Zhang Z (2000) Intrastriatal transplantation of bone marrow nonhematopoietic cells improves functional recovery after stroke in adult mice. *J Cereb Blood Flow Metab* 20:1311–9

Lin Y, Liu L, Li Z, Qiao J, Wu L, Tang W, Zheng X, Chen X, Yan Z, Tian W (2006) Pluripotency potential of human adipose-derived stem cells marked with exogenous green fluorescent protein. *Mol Cell Biochem* 291:1–10

Lindvall O, Kokaia Z (2006) Stem cells for the treatment of neurological disorders. *Nature* 441:1094–6

Loos M, Dihne M, Block F (2003) Tumor necrosis factor-alpha expression in areas of remote degeneration following middle cerebral artery occlusion of the rat. *Neuroscience* 122:373–80

Lu P, Blesch A, Tuszynski MH (2004) Induction of bone marrow stromal cells to neurons: differentiation, transdifferentiation, or artifact? *J Neurosci Res* 77:174–91

Lundkvist J, Lendahl U (2001) Notch and the birth of glial cells. *Trends Neurosci* 24:492–4

Mimura T, Dezawa M, Kanno H, Yamamoto I (2005) Behavioral and histological evaluation of a focal cerebral infarction rat model transplanted with neurons induced from bone marrow stromal cells. *J Neuropathol Exp Neurol* 64:1108–17

Morris R (1984) Developments of a water-maze procedure for studying spatial learning in the rat. *J Neurosci Methods* 11:47–60

Nguyen TH, Khakhoulina T, Simmons A, Morel P, Trono D (2005) A simple and highly effective method for the stable transduction of uncultured porcine hepatocytes using lentiviral vector. *Cell Transplant* 14:489–96

Ohta T, Kikuta K, Imamura H, Takagi Y, Nishimura M, Arakawa Y, Hashimoto N, Nozaki K (2006) Administration of ex vivo-expanded bone marrow-derived endothelial progenitor cells attenuates focal cerebral ischemia-reperfusion injury in rats. *Neurosurgery* 59:679–86; Discussion -86

Prockop DJ (1997) Marrow stromal cells as stem cells for nonhematopoietic tissues. *Science* 276:71–4

Puurunen K, Jolkkonen J, Sirvio J, Haapalinna A, Sivenius J (2001) Selegiline combined with enriched-environment housing attenuates spatial learning deficits following focal cerebral ischemia in rats. *Exp Neurol* 167: 348–55

Reubinoff BE, Itsykson P, Turetsky T, Pera MF, Reinhartz E, Itzik A, Ben-Hur T (2001) Neural progenitors from human embryonic stem cells. *Nat Biotechnol* 19:1134–40

Shen LH, Li Y, Chen J, Cui Y, Zhang C, Kapke A, Lu M, Savant-Bhonsale S, Chopp M (2007) One-year follow-up after bone marrow stromal cell treatment in middle-aged female rats with stroke. *Stroke* 38:2150–6

Shimizu S, Kitada M, Ishikawa H, Itokazu Y, Wakao S, Dezawa M (2007) Peripheral nerve regeneration by the in vitro differentiated-human bone marrow stromal cells with Schwann cell property. *Biochem Biophys Res Commun* 359:915–20

Takagi Y, Nishimura M, Morizane A, Takahashi J, Nozaki K, Hayashi J, Hashimoto N (2005) Survival and differentiation of neural progenitor cells derived from embryonic stem cells and transplanted into ischemic brain. *J Neurosurg* 103:304–10

Tang Y, Yasuhara T, Hara K, Matsukawa N, Maki M, Yu G, Xu L, Hess DC, Borlongan CV (2007) Transplantation of bone marrow-derived stem cells: a promising therapy for stroke. *Cell Transplant* 16:159–69

Veizovic T, Beech JS, Stroemer RP, Watson WP, Hodges H (2001) Resolution of stroke deficits following contralateral grafts of conditionally immortal neuroepithelial stem cells. *Stroke* 32:1012–9

Yanagisawa D, Qi M, Kim DH, Kitamura Y, Inden M, Tsuchiya D, Takata K, Taniguchi T, Yoshimoto K, Shimohama S, Akaike A, Sumi S, Inoue K (2006) Improvement of focal ischemia-induced rat dopaminergic dysfunction by striatal transplantation of mouse embryonic stem cells. *Neurosci Lett* 407:74–9

Yonemori F, Yamaguchi T, Yamada H, Tamura A (1999) Spatial cognitive performance after chronic focal cerebral ischemia in rats. *J Cereb Blood Flow Metab* 19:483–94

Supplementary Information accompanies the paper on the Journal of Cerebral Blood Flow & Metabolism website (http://www.nature.com/jcbfm)

Experimental Neurology xxx (2010) xxx–xxx

Contents lists available at ScienceDirect

Experimental Neurology

journal homepage: www.elsevier.com/locate/yexnr

Long-term observation of auto-cell transplantation in non-human primate reveals safety and efficiency of bone marrow stromal cell-derived Schwann cells in peripheral nerve regeneration

Shohei Wakao [a,1], Takuya Hayashi [b,1], Masaaki Kitada [a,1], Misaki Kohama [a], Dai Matsue [a], Noboru Teramoto [b], Takayuki Ose [b], Yutaka Itokazu [c], Kazuhiro Koshino [b], Hiroshi Watabe [b], Hidehiro Iida [b], Tomoaki Takamoto [d], Yasuhiko Tabata [d], Mari Dezawa [a,*]

[a] Department of Stem Cell Biology and Histology, Tohoku University Graduate School of Medicine, Sendai 980-8575, Japan
[b] Department of Investigative Radiology, Advanced Medical Engineering Center, National Cardiovascular Center Research Institute, Osaka 565-8565, Japan
[c] Department of Anatomy and Neurobiology, Kyoto University Graduate School of Medicine, Kyoto 606-8501, Japan
[d] Department of Biomaterials, Field of Tissue Engineering, Institute for Frontier Medical Sciences, Kyoto University, Kyoto 606-8507, Japan

ARTICLE INFO

Article history:
Received 19 November 2009
Revised 25 January 2010
Accepted 29 January 2010
Available online xxxx

Keywords:
Mesenchymal stem cells
Monkey
Schwann cells
Nerve regeneration
Peripheral nerve
Transdifferentiation

ABSTRACT

Based on their differentiation ability, bone marrow stromal cells (MSCs) are a good source for cell therapy. Using a cynomolgus monkey peripheral nervous system injury model, we examined the safety and efficacy of Schwann cells induced from MSCs as a source for auto-cell transplantation therapy in nerve injury. Serial treatment of monkey MSCs with reducing agents and cytokines induced their differentiation into cells with Schwann cell properties at a very high ratio. Expression of Schwann cell markers was confirmed by both immunocytochemistry and reverse transcription-polymerase chain reaction. Induced Schwann cells were used for auto-cell transplantation into the median nerve and followed-up for 1 year. No abnormalities were observed in general conditions. Ki67-immunostaining revealed no sign of massive proliferation inside the grafted tube. Furthermore, ^{18}F-fluorodeoxygluocose-positron emission tomography scanning demonstrated no abnormal accumulation of radioactivity except in regions with expected physiologic accumulation. Restoration of the transplanted nerve was corroborated by behavior analysis, electrophysiology and histological evaluation. Our results suggest that auto-cell transplantation therapy using MSC-derived Schwann cells is safe and effective for accelerating the regeneration of transected axons and for functional recovery of injured nerves. The practical advantages of MSCs are expected to make this system applicable for spinal cord injury and other neurotrauma or myelin disorders where the acceleration of regeneration is expected to enhance functional recovery.

Introduction

Schwann cells are peripheral glial cells that form the myelin of the peripheral nervous system (PNS) and have a major role in neuronal function including saltatory conduction. Following PNS injury, Schwann cells have a pivotal role in axonal degeneration and regeneration. During Wallerian degeneration, myelin is degraded and Schwann cells are activated and proliferate to produce a variety of neurotrophic factors, cytokines, and cell adhesion molecules, thereby providing a pathway for regenerating axons (Fawcett and Keynes, 1990; Hall, 2001; Radtke and Vogt, 2009; Torigoe et al., 1996). Schwann cells have a crucial role in the endogenous repair of the PNS by reconstructing myelin, which is indispensable for neurologic function. Schwann cells also support reconstruction of the injured central nervous system (CNS) where successful axonal regeneration and functional reconstruction are not normally achieved by oligodendrocytes (Dezawa and Adachi-Usami, 2000). Several experiments in the spinal cord and some other areas in the CNS have shown that the injection or transplantation of cultured Schwann cells induces axonal growth across the site of injury and contributes to functional recovery (Bunge, 2002; Bunge, 2008; Hill et al., 2006; Plant et al., 1998; Vukovic et al., 2007). For these reasons, Schwann cells have long attracted attention and are thus one of the most widely studied cell types for axonal regeneration both in the PNS and CNS.

Although Schwann cells have a strong ability to induce nerve regeneration, it is difficult to obtain a sufficient amount of Schwann cells for clinical use. Schwann cell cultivation requires another peripheral nerve being newly sacrificed. In addition, several technical

* Corresponding author. Department of Stem Cell Biology and Histology, Tohoku University Graduate School of Medicine, 2-1 Seiryo-machi, Aoba-ku, Sendai 980-8575, Japan. Fax: +81 22 717 8030.
E-mail address: mdezawa@m.tains.tohoku.ac.jp (M. Dezawa).
[1] These authors contributed equally.

0014-4886/$ – see front matter © 2010 Elsevier Inc. All rights reserved.
doi:10.1016/j.expneurol.2010.01.022

difficulties remain for harvesting and expanding a large number of Schwann cells. Accordingly, it is desirable to establish cells with Schwann cell characteristics from sources other than the PNS that are easy to access, capable of rapid expansion, amenable to survival, and able to integrate into the host tissue to elicit axonal regeneration and to contribute to re-myelination.

Therefore, we previously used bone marrow stromal cells (MSCs) as a source for inducing Schwann cells because MSCs are easily accessible through aspiration of the bone marrow from patients or a marrow bank and can be expanded in culture with fewer ethical problems compared to other sources. MSCs can be readily expanded in large scale for auto-transplantation, and have the potential to differentiate into other kinds of cells such as osteoblasts, adipocytes, and chondrocytes (Pittenger et al., 1999; Prockop, 1997).

Induction of Schwann cells from MSCs is efficiently achieved by first reverting human and rodent MSCs to an undifferentiated state using beta-mercaptoethanol (BME) followed by retinoic acid (RA) treatment and then inducing differentiation by treating them with forskolin (FSK), basic fibroblast growth factor (bFGF), platelet-derived growth factor (PDGF), and neuregulin, all of which are factors related to Schwann cell differentiation (Dezawa et al., 2001). The induced cells are different from the original untreated MSCs, but are morphologically quite similar to Schwann cells and express Schwann cell markers at a high ratio (Dezawa et al., 2001). The effectiveness of this induction system was also demonstrated by other groups in other mesenchymal stem cells such as adipose-derived stem cells (Jiang et al., 2008; Kingham et al., 2007; Xu et al., 2008).

It is noteworthy that human and rodent MSC-derived Schwann cells express myelin-related markers and contribute to re-myelination when transplanted into rat sciatic nerve injury (Mimura et al., 2004; Shimizu et al., 2007), and also effectively promote axonal regeneration and functional recovery in spinal cord injury (Kamada et al., 2005; Someya et al., 2008). These findings demonstrate that MSC-derived Schwann cells are effective for both PNS and CNS regeneration.

To extend this system to clinical application, the safety and effectiveness in higher mammals must be evaluated. The potential for auto-cell transplantation is one of the strong advantages of MSCs. In this study, we estimated the safety and effectiveness of MSC-derived Schwann cells for auto-cell transplantation in a PNS injury model in cynomolgus monkey. The expression of Schwann cell markers in the MSC-derived Schwann cells was confirmed by both immunocytochemistry and reverse transcription-polymerase chain reaction (RT-PCR). Artificial grafts were made by transferring MSC-derived Schwann cells into trans-permeable tubes filled with 3-dimensional collagen, transplanted into the gap between transected median nerve segments, and followed-up for 1 year. No abnormalities were observed in general conditions. In ^{18}F-fluorodeoxygluocose (FDG)-positron emission tomography (PET) scanning, which allows for highly sensitive detection of neoplastic cells, no abnormal accumulation of radioactivity was observed except in regions known to have physiologic accumulations. Cell proliferation assessed by Ki67 immunostaining demonstrated no mass formation and low proliferation of cells. Restoration of the transplanted nerve was confirmed by the hand movement analysis, electrophysiology, and histology.

These results suggest that auto-cell transplantation therapy using MSC-derived Schwann cells is effective and is very likely to be safe for nerve injury. The practical advantages of MSCs is expected to make this system applicable for treatment of spinal cord injury and other neurotrauma or neurodegenerative diseases where Schwann cell transplantation is expected to be effective.

Materials and methods

Animal experiments using cynomolgus monkeys were approved by the Animal Care and Experimentation Committee of the Kyoto University Graduate School of Medicine, Tohoku University Graduate School of Medicine and the National Cardiovascular Center Research Institute. Six adult male cynomolgus monkeys (3 to 4 years of age) were used in this experiment. Cynomolgus monkeys have been broadly used to evaluate the efficiency of transplantation methods particularly in PNS injury models (Ahmed et al., 1999; Archibald et al., 1995; Auba et al., 2006; Hess et al., 2007; Lee et al., 2008). Furthermore, we have previously confirmed the transdifferentiation capacity of MSCs in cynomolgus monkeys, i.e., to be induced into neuronal cells (Nagane et al., 2009). For these reasons, we chose cynomolgus monkeys as the experimental animal in this study.

Isolation of monkey MSCs and Schwann cell induction

Primary monkey MSCs were isolated from the pelvic bone. Bone marrow aspirate (5 ml) was diluted 1:10 using culture medium comprised of alpha-minimum essential medium (MEM), 15% fetal bovine serum (FBS), 2 mM L-glutamine, and kanamycin and incubated at 37 °C, 5% CO_2. After 4 days, non-adherent cells were removed by replacing the medium. Adherent MSCs were expanded when they reached 95% confluence, and were subcultured 4 times, and then finally subjected to the Schwann cell induction.

MSCs were subcultured at a density of 1.76×10^3 cells/cm^2 and incubated in alpha-MEM containing 1 mM BME without serum for 24 h. The culture medium was then replaced with alpha-MEM containing 10% FBS and 35 ng/ml all-trans-RA (Sigma, St. Louis, MO). Three days later, cells were transferred to alpha-MEM containing 10% FBS, 5 μM FSK (Calbiochem, La Jolla, CA), 10 ng/ml bFGF (Peprotech, London, UK), 5 ng/ml PDFG-AA (Peprotech, London, UK), and 200 ng/ml heregulin-ß1-EGF-domain (R&D Systems, Minneapolis, MN) and cultured for 4 to 5 days. These Schwann cells induced from MSCs were called 'M-Schwann cells' in the following sections.

Evaluation of M-Schwann cells

M-Schwann cells were evaluated using both phase-contrast microscopic observation and immunocytochemistry. For immunocytochemistry, the YST-1 cell line was used for positive control (RIKEN, Ibaraki, Japan), monkey naïve MSCs as a negative control, and monkey M-Schwann cells were fixed with 4% paraformaldehyde in 0.02 M phosphate buffered saline (PBS). Primary antibodies used for the immunocytochemistry were anti-protein zero (P0) rabbit IgG (1:300, kindly provided by Dr. J.J. Archelos, Karl-Franzens Universitat, Graz, Austria), anti-p75 (nerve growth factor receptor) mouse IgG (1:500, Abcam Cambridge, UK), anti-glial fibrillary acidic protein (GFAP) rabbit IgG (1:300, DAKO, Carpinteria, CA), anti-O4 mouse IgM (1:20, Boehringer Ingelheim GmbH, Ingelheim, Germany), anti-CD90 mouse IgG (1:400, BD Bioscience, Bedford, MA), and anti-smooth muscle actin (SMA) mouse IgG (1:400, LabVision, Newmarket, Suffolk, UK). These primary antibodies were detected by Alexa 568-conjugated anti-rabbit IgG, anti-mouse IgG, or anti-mouse IgM antibodies (Molecular Probes, Invitrogen, Carlsbad, CA). Immunocytochemistry was performed as previously described (Kitada et al., 2001). Briefly, samples were incubated in 20% BlockAce (skim milk, Yukijirushi, Tokyo, Japan) in 0.005% saponin and 50 mM glycine in PBS (SaGlyPBS) for 10 min, incubated with the primary antibody in 5% BlockAce in SaGlyPBS overnight at 4 °C followed by the secondary antibody incubation in 5% BlockAce in SaGlyPBS. Nuclei were counterstained with 4′, 6-diamidino-2-phenylindole (DAPI, Molecular Probes). As for immunostaining against CD90, cells were incubated with anti-CD90 antibody in culture medium at 37 °C, 5% CO_2, washed, fixed with 4% paraformaldehyde in 0.02 M PBS, and further processed for secondary antibody incubation. All images were taken by a confocal laser scanning microscope (CS-1, Nikon, Kawasaki, Japan) with the same laser intensity and detection sensitivity.

Please cite this article as: Wakao, S., et al., Long-term observation of auto-cell transplantation in non-human primate reveals safety and efficiency of bone marrow stromal cell-derived Schwann..., Exp. Neurol. (2010), doi:10.1016/j.expneurol.2010.01.022

Expression of Schwann cell markers in RT-PCR

Total RNA from naïve MSCs and M-Schwann cells was extracted using an RNeasy Mini Kit (Qiagen GmbH, Hilden, Germany) and purified in accordance with the manufacturer's instructions. From 1 μg of total RNA, first-strand cDNA was generated using SuperScript II reverse transcriptase (Invitrogen, Carlsbad, CA). The PCR reactions were performed using Ex Taq DNA polymerase (TaKaRa, Tokyo, Japan). The amplification conditions were: 1 min at 94 °C, 1 min at 60 °C, and 1 min at 72 °C, for 30 cycles (25 cycles for β-actin) and a final incubation at 72 °C for an additional 7 min.

We used the following *Macaca fascicularis* PCR Primers that are specific genes for Schwann cells, and β-actin as internal control. ß-actin sense: 5′-TCTAGGCGGACTGTGACTTAGTTGCGTTAC-3′ and antisense: 5′-AATCAAAGTCCTCGGCCACATTGTAGAACT-3′, GFAP sense: 5′-TGCCCTAGGCTCCATCAGTATT-3′ and antisense: 5′-TCCCAGATACC-CTGAGAGAACCT-3′, Krox20 sense: 5′-AGTACCCCAACAGACCTAG-CAAGA-3′ and antisense: 5′-GCAAACTTTCGGCCACAGTAG-3′, MBP sense: 5′-CCCACACACCCCAATTAGCT-3′ and antisense: 5′-GCATCAC-GCTGACTACTCCTCAT-3′.

M-Schwann cell autologous PNS graft

The composition and construction of the biodegradable conduit and collagen sponge were previously reported (Hisasue et al., 2005). Briefly, the copolymer was composed of 75% L-lactic acid and 25% E-caprolactone. A rotating polytetrafluoroethylene tube 2 mm in diameter was dipped in the copolymer solution, immersed in liquid nitrogen for a few minutes, and air dried at 25 °C for 24 h. The tube used for transplantation was 4 mm long with 2-mm internal and 3-mm external diameters. A solid sample of atelocollagen (Nippon Meat Packers, Osaka, Japan; 70 wt.% type I and 30 wt.% type III collagen) was used for sponge preparation. Atelocollagen was dissolved in HCl aqueous solution to a final concentration of 1.0 wt.%. The collagen solution was whipped on a homogenizer, frozen at −80 °C, and freeze-dried. Collagen sponge was prepared by cutting it into pieces to fill the biodegradable conduit. The fabricated guide tubes and collagen sponge were sterilized with ethylene oxide gas before use. This artificial conduit can hold cells or tissue, which will be a scaffold for supporting axonal regeneration. Also, this artificial conduit is gas permeable so that cells inside the graft are able to survive after transplantation (Mligiliche et al., 2003).

To determine the cell concentration of the artificial grafts, we inspected normal monkey median nerve sections by Giemsa staining. We calculated 250 myelinated axons were contained within an area of 110 μm^2, suggesting 250 Schwann cells are myelinating axons in this square measure. The total transverse area of the monkey median nerve, except for the epineurium, was approximately 1570 μm^2. Based on the average length of a Ranvier's node (~1000 μm), a 1-cm nerve segment is estimated to contain approximately 2×10^6 Schwann cells. Thus, the tube was filled with induced M-Schwann cells at a concentration of 2×10^6 cells suspended in 30-μl 0.01 M PBS per 1-cm tube and incubated in 10% FBS containing alpha-MEM for several hours in 5% CO2 at 37 °C before transplantation. The graft was longitudinally cut and counterstained with Hoechst 33342 to observe the distribution of the cells inside the graft.

Transplantation of autologous M-Schwann cell grafts to median nerve

We chose the median nerve to make the PNS injury model, because this nerve is relatively easily accessible and the function of this nerve is easier to evaluate during the regenerative period, rather than any other nerves in cynomolgus monkey (Archibald et al., 1995). Just before transplantation, the motor nerve conduction study (described below) was performed under ketamine- and xylazine-induced general anesthesia. A 20-mm segment of unilateral median nerve was completely removed 2 cm proximal to the wrist joint of the forearm and the artificial graft was anastomosed to the proximal and distal nerve tips and their neurilemma using 10-0 nylon sutures at both ends. Five monkeys (M-Schwann cell-transplanted group) received auto-cell transplantation of the M-Schwann cells, while two monkeys (the sham-operated group) received transplantation of empty artificial grafts that were not filled with M-Schwann cells. Just after transplantation, a motor nerve conduction study performed again to confirm the absence of CMAP indicated that the median nerve was completely transected. For auto-cell transplantation, M-Schwann cells were all derived from each recipient animal so that no immunosuppression was given after transplantation.

General health and behavior analyses

Weight check and blood tests (urea nitrogen, creatinine, creatine phosphokinase, aspartate amino transferase, alanine transferase, lactate dehydrogenase, platelet, hemoglobin, red blood cells, white blood cells, hematocrit, mean corpuscular volume, mean corpuscular hemoglobin, mean corpuscular hemoglobin concentration, D-dimer and fibrinogen A) were performed every month before and after transplantation.

For behavioral analysis, movements of the hand and thumb, and grip strength for obtaining food of both the transplanted and intact sides were recorded on a video tape and analyzed for evaluation. The criteria for hand motion and functional recovery scores were as follows:

Score 5: Strength of the thumb, hand movement, and frequency of hand use for feeding and general behavior, such as grabbing the cage, are nearly equal between operated and intact sides.

Score 4: Strength of the thumb is asymmetrical, but the frequency of the use of the hands is nearly the same in both sides. Monkey is able to grab, but is unable to pinch small objects less than 1 cm.

Score 3: Monkey can grab the cage, but muscular force of the operated hand is weak. The thumb is contractured. Wrist movement compensates for the weakness of the hand and thumb. The muscle force of the thumb is less than half that of the intact side.

Score 2: Functional recovery is weak. Movement of the thumb is observed, but compensation by the wrist is recognized. The use of the operated hand during feeding is rare.

Score 1: Little hand and finger motion on the operated side. Monkey is unable to grab objects.

Score A: Unmeasurable. Monkey is unable to make contact because of too much guarding.

The evaluation was conducted by a person, who did not operate animals, without any information about the animal including the procedure of transplantation, and the observation period after the transplantation.

Motor nerve conduction study

To estimate the restoration of nerve function, we performed motor nerve conduction study at five time points for each animal, just before and after transplantation and at 3, 6, and 12 months after the transplantation. To record the compound muscle action potential (CMAP) in the motor nerve conduction study, we pasted the anode electrode plate on the skin of the palmar side at the proximal joint of the first digit, the cathode electrode plate on the belly muscle of the abductor pollicis brevis, and the ground plate on the back of the forearm (Someya et al., 2008). The median nerve was stimulated with a rectangular wave-shaped pulse using a bipolar stimulator by placing its cathode at either of the following sites; 5-cm proximal to the wrist joint (3 cm proximal to the transplanted site) and at the cubital fossa. At each stimulation site, we applied electrical current of supramaximal intensity (varying from 5 mA to 25 mA) within a range that did not induce ulnar nerve stimulation. For each study, we recorded the CMAP, distal latency (time latency between the stimulus

Please cite this article as: Wakao, S., et al., Long-term observation of auto-cell transplantation in non-human primate reveals safety and efficiency of bone marrow stromal cell-derived Schwann..., Exp. Neurol. (2010), doi:10.1016/j.expneurol.2010.01.022

at the wrist and the increase in the CMAP), and the distance (the length between the recording electrode and the stimulator at the wrist). We used the amplitude of the CMAP and distal velocity (distal latency divided by the distance) for further analysis. For the motor nerve conduction study, we used an EMG/evoked potential measuring system (Neuropack μ, MEB-9100, Nihon Koden, Tokyo, Japan). We used SPSS (ver. 12.0, SPSS Inc., Chicago, IL) for the statistical analysis.

PET using ^{18}F-FDG

For the ^{18}F-FDG-PET scan, we injected ~185 MBq of ^{18}F-FDG produced at the National Cardiovascular Center Research Institute using a conventional method described previously (Hamacher et al., 1986) and scanned the whole body for 48 min starting at 60 min after the injection. For the PET scan, we used a PET scanner (PCT-2000A, Toshiba Medical Systems Corp, Tokyo, Japan) that provided 47 slices in an axial field of view of 162 mm with an intrinsic resolution of 6.2 mm (trans-axial) and 6.0 mm (axial) in full-width-at-half-maximum. The scan was performed in a three-dimensional mode after the transmission scan using three rotating ^{68}Ga–^{68}Ge rod sources. The images were reconstructed in a matrix of $128 \times 128 \times 223$ (x, y, z) with a voxel size of $5.15 \times 5.15 \times 5.15$ mm (x, y, z) using a filtered back projection algorithm. The reconstructed ^{18}F-FDG radioactivity image (in Bq/ml) was scaled by the injected dose of ^{18}F-FDG per body weight of animal (Bq/g) to calculate images of SUV. The region was considered to be abnormal when the SUV value was greater than 2.5 (Al-Sugair and Coleman, 1998), and when located in the area outside of organs known to have physiologic accumulation of FDG (brain, heart, urinary tracts, and kidneys). SUV images were inspected by coronal, axial, and sagittal sections and also by the maximum intensity projection.

Immunohistochemical analysis of transplanted grafts

One year after transplantation, animals were sacrificed by an overdose of pentobarbital and perfused transcardially with 4% paraformaldehyde in 0.01 M PBS. The transplanted median nerve, including the proximal site, graft, and distal site, was dissected out and incubated in the same fixative for 6 h at 4 °C. Tissues were washed with 0.1 M PBS overnight at 4 °C, immersed in 10%, 20%, and 30% sucrose–PBS for 3 h each at 4 °C, embedded in OCT, and cut into 10-μm-thick frozen sections using a cryostat. Immunohistochemistry was performed as described elsewhere (Kitada et al., 2001). Primary antibodies used for immunohistochemistry were: anti-neurofilament (NF) rabbit polyclonal antibody (Sigma), anti-myelin-associated glycoprotein (MAG) mouse monoclonal antibody (1:100, Boehringer Ingelheim, Ingelheim am Rhein, Germany), anti-Ki67 rabbit monoclonal SP-6 IgG (1:300), and anti-CD163 mouse monoclonal IgG (1:20, Hycult Biotechnology, Uden, Netherlands). Secondary antibodies were: anti-rabbit IgG conjugated to Alexa488 (Molecular Probes) and anti-rabbit or anti-mouse IgG conjugated to Alexa568 (Molecular Probes). To assess the extent of regeneration, the ratio of the NF-positive area inside the grafted tube at the middle of the graft was calculated in three 10-μm-thick transverse sections from each animal. Statistical analysis of the ratio of NF-positive area to the total nerve area was compared using ANOVA with pairwise comparison using *t*-tests. To analyze the distribution of proliferating cells inside the grafted tube, immunostaining against Ki67 was done under the antigen retrieval technique using microwave (Kitada and Rowitch, 2006).

Results

Schwann cell induction from cynomolgus monkey MSCs

Cultured naïve MSCs of cynomolgus monkey are shown in Fig. 1A. When naïve MSCs were treated with BME followed by RA administration, and a set of cytokines (bFGF, FSK, PDGF, and neuregulin), their morphology changed similar to human and rat M-Schwann cells (Figs. 1B–D), suggesting the possibility of Schwann cell induction from monkey MSCs. Cells exhibiting morphological changes were evaluated to determine whether they had acquired Schwann cell phenotypes. In immunocytochemistry, Schwann cell markers including p75, GFAP, P0, and O4 became positive in monkey M-Schwann cells, while naïve MSCs or M-Schwann cells without primary antibody incubation (data not shown) showed no immunoreactivity against

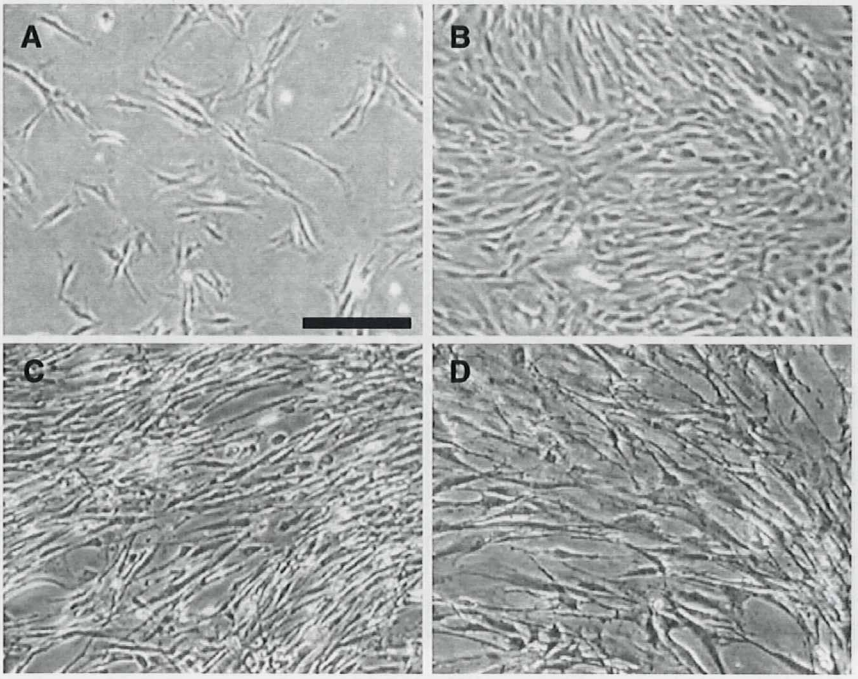

Fig. 1. Phase contrast microscopy. A: Naïve monkey MSCs, B: monkey M-Schwann cells, C: human M-Schwann cells, and D: rat M-Schwann cells. Morphological changes were evident from A to B. M-Schwann cells derived from human and rat exhibited similar morphology to those from monkey. Scale bar: 30 μm.

Please cite this article as: Wakao, S., et al., Long-term observation of auto-cell transplantation in non-human primate reveals safety and efficiency of bone marrow stromal cell-derived Schwann..., Exp. Neurol. (2010), doi:10.1016/j.expneurol.2010.01.022

these Schwann cells markers (Fig. 2). Schwann cell markers analyzed were all positive in the YST-1 cells. The rate of p75-positive cells in M-Schwann cells was estimated to be 99.0 ± 0.01% (mean ± SD). RT-PCR showed the mRNA expression of GFAP and Krox20 was weakly detected in naïve MSCs, but was up-regulated following M-Schwann cell induction. Myelin basic protein (MBP), another marker for Schwann cells, was undetectable in naïve MSCs but became clearly detectable in M-Schwann cells (Fig. 3). These results suggested that M-Schwann cells expressed markers and factors related to Schwann cell properties. We tried to determine whether M-Schwann cells sustained their expression of MSC markers such as CD90 and SMA (Supplementary Fig. 1). Whereas CD90 was not expressed in M-Schwann cells, SMA expression was recognized and the expression level of SMA was varied in each M-Schwann cell. These findings suggest that M-Schwann cells might partially trail some of the MSC characteristics at least in culture, although it is unknown whether M-Schwann cells lose or retain the MSC property during maturation in the transplanted environment.

Prior to transplantation, we constructed the graft tube made with lactic acid and E-caprolactone and filled the inside of the graft tube with collagen sponge and M-Schwann cells (see Materials and methods). Cell number was calculated to mimic endogenous Schwann cell number in an intact monkey peripheral nerve. To observe the distribution of the cells inside the graft, the graft was longitudinally cut and the nuclei of the cells were counterstained with Hoechst 33342 (Supplementary Fig. 2). Nuclei of the cells were homogenously distributed inside the graft.

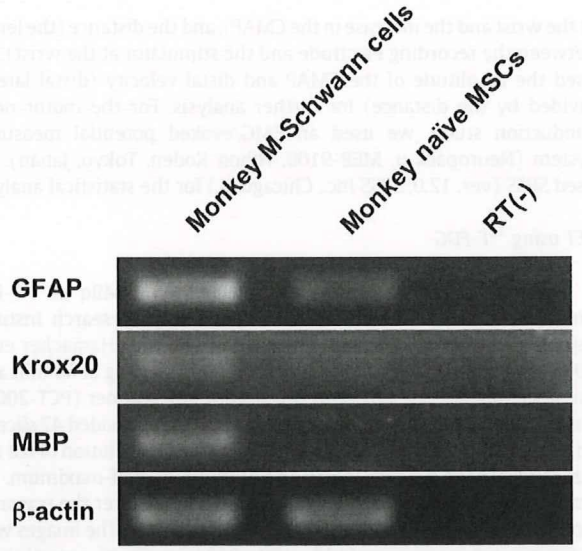

Fig. 3. RT-PCR of Schwann cell markers. Naïve MSCs slightly expressed for mRNA of GFAP and Krox20, but did not express that of myelin basic protein (MBP). Monkey M-Schwann cells, however, presented up-regulation of GFAP and Krox20 mRNA, and became clearly positive for MBP.

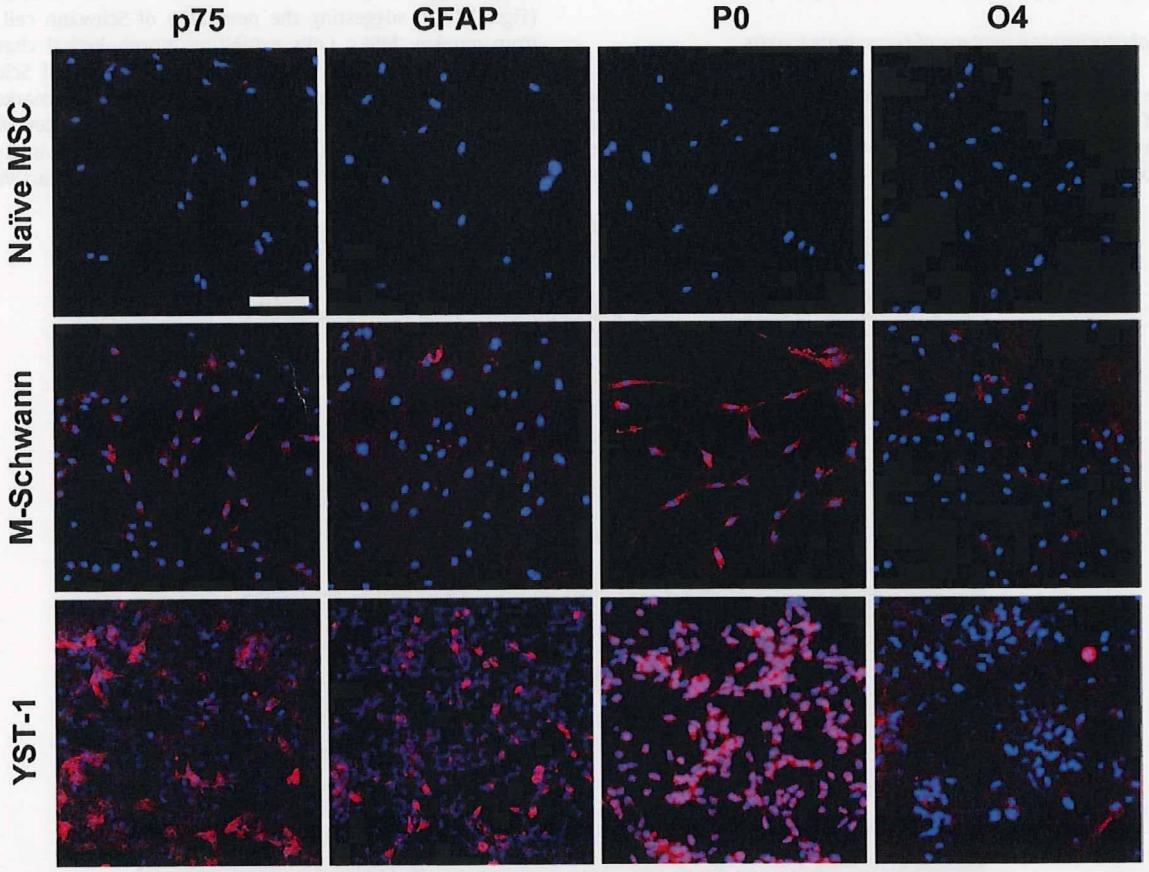

Fig. 2. Immunocytochemistry of naïve MSCs and M-Schwann cells. Initially naïve MSCs exhibited almost no immunoreactivity for Schwann cell markers (red) such as p75, GFAP, P0, and O4. After induction of Schwann cells, M-Schwann cells were positive for all Schwann cell markers: p75, GFAP, P0, and O4. YST-1 was used as a positive control and was also positive for all Schwann cells markers analyzed. DAPI (blue) was used for the counterstaining of nuclei. Scale bar: 50 μm.

Please cite this article as: Wakao, S., et al., Long-term observation of auto-cell transplantation in non-human primate reveals safety and efficiency of bone marrow stromal cell-derived Schwann..., Exp. Neurol. (2010), doi:10.1016/j.expneurol.2010.01.022

Table 1
Body weight (kg).

Group	Animal	Pre	3 m	6 m	12 m
M-Schwann cell-transplanted group	mon0038	4.2	5.1	5.5	5.4
	mon0039	4.8	5.3	5.3	4.9
	mon0044	3.8	4.3	4.5	4.9
	mon0046	3.8	4.3	4.7	4.5
Sham-operated group	mon0045	4.1	4.5	4.8	5.0
	mon0050	3.7	2.8	2.8	3.7

Body weight (kg) is shown at four time points: before transplantation (pre), and at 3, 6, and 12 months after transplantation (3 m, 6 m, and 12 m, respectively).

Table 3
Scores for hand motion recovery.

Group	Animal	3 m	6 m	9 m	12 m
M-Schwann cell-transplanted group	mon0038	3	4	5	5
	mon0039	3	4	5	5
	mon0044	4	4	5	5
	mon0046	4	A	4	4
Sham-operated group	mon0045	1	1	2	2
	mon0050	A	A	1	1

Scores for hand motion recovery at 3, 6, 9, and 12 months after surgery. In the sham-operated group, score 2 was the highest score achieved at 1 year, whereas the M-Schwann cell-transplanted group showed good recovery up to score 5.

General health follow-up

Grafts filled with autologous M-Schwann cells were transplanted to the unilateral median nerve in the M-Schwann cell-transplanted group (monkey numbers: mon0038, mon0039, mon0044, and mon0046). For the sham-operated group, tubes without cells were transplanted (monkey numbers: mon0045 and mon0050). Motor nerve conduction velocity was measured just before and after transplantation to confirm the complete transection of the median nerve.

For follow-up of general health, body weight check and blood tests were performed at 1 to 6 month intervals after transplantation. In both the M-Schwann cell-transplanted and sham-operated groups, no considerable weight loss was observed, except in one animal in the sham-operated group (mon0050; Table 1). Creatinine, creatine kinase, glutamate oxaloacetate transaminase, glutamate pyruvate transaminase, lactate dehydrogenase, platelet, hemoglobin, red blood cell, and white blood cell levels were within normal range in the M-Schwann cell-transplanted group. Blood urea nitrogen was slightly elevated (Table 2). The animals in the sham-operated group also showed elevated blood urea nitrogen and glutamate oxaloacetate transaminase, glutamate pyruvate transaminase, and lactate dehydrogenase higher than normal values. Although the normal values of D-dimer and fibrinogen A are not established in the intact cynomolgus monkeys, the values were almost within the normal range of humans and did not increase during the follow-up period in either group.

Behavioral analysis

To assess functional recovery, general behavior, hand motion, and movement of muscles along the distribution of the affected median nerve were video-recorded and evaluated to be in 5 levels (see Materials and methods). The functional recovery score of the M-Schwann cell-transplanted group was high at 3 months while that of the sham-operated group was markedly lower even at 1 year. In the sham-operated group, because the use frequency was very low, and hand motion or food grabbing were poor due to the rigidity of the operated hand, their scores remained around 1 and 2. The M-Schwann cell-transplanted group had a mean functional recovery score of approximately 3 and 4 at 6 months. At 9 and 12 months, some monkeys in the M-Schwann cell-transplanted group achieved the highest possible score of 5 (Table 3). Actual hand movements used in feeding are shown in the video-recorded data (see movies in Supplementary information).

Any animals both in the sham-operated and M-Schwann cell-transplanted groups did not exhibit self-mutilation or overgrooming in the radial palm of the hand, the innervation area of sensory branch of the transected median nerve, suggesting no abnormal sensation including dysethesia or hyperalgesia was evoked by transplanted tube and M-Schwann cells.

Motor nerve conduction study

We analyzed the amplitude of the CMAP and the distal velocity, both measured in each animal at five time points (just before and after transplantation, and 3, 6, and 12 months after transplantation; Fig. 4). The group comparison at each observation period was done by the two sample sign test, showing significant differences at 6 and 12 months after transplantation between the M-Schwann cell-transplanted and sham-operated groups. At 12 months after transplantation, the CMAP in M-Schwann cell-transplanted group nerves recovered to ~60% (mean ± SD = 7.27 ± 4.41 mV) than that of the pre-transplanted nerves (12.2 ± 0.73 mV). The sham-operated CMAP reached ~20% (2.45 ± 0.51 mV). The whole data of each experimental group was further analyzed by the two-way repeated analysis of variance (repeated ANOVA) with factors of group (M-Schwann cell-transplanted vs. sham-operated) and the observation period and found a significant effect of group in CMAP. The M-Schwann cell-transplanted group had a significantly greater CMAP ($F_{1,4} = 5.02$, one-

Table 2
Results of the blood analysis.

	M-Schwann cell-transplanted group ($n=4$)				Sham-operated group ($n=2$)				Normal values ($n=27$)
	Post-1	Post-2	Post-3	Post-4	Post-1	Post-2	Post-3	Post-4	
WBC ($\times 10^2$/μl)	116 (19)	123 (27)	107 (17)	88 (14)	122 (17)	111 (1)	117 (6)	77 (53)	133 (57)
RBC ($\times 10^4$/μl)	554 (50)	567 (59)	565 (51)	576 (56)	562 (10)	580 (5)	497.5 (67)	540 (18)	587(77)
Hb (g/dL)	13.1 (0.5)	13.5 (0.8)	13.25 (0.5)	13.7 (1.5)	13.0 (0.3)	13.5 (0.4)	12.9 (0.8)*	12.6 (0.1)	14.6(1.1)
PLT ($\times 10^4$/μl)	35.4 (14.0)	32.5 (10.0)	30.2 (7)	32.5 (11)	38.0 (3.6)	31.0 (0.1)	31.5 (0.5)	30.2 (5.0)	37.9(10.8)
GOT (IU/L)	29 (5)	28 (3)	29 (4)	36 (6)	32 (2)	46 (9)*	38 (5)	25 (1)	31(8)
GPT (IU/L)	15 (1)	26 (3)	27 (5)	34 (7)	31 (21)	64 (33)*	64 (7)**	30 (5)	36(12)
LDH (IU/L)	437 (182)	337 (30)	377 (25)	479 (116)	343 (80)	511 (123)	401 (62)	265 (35)	592(116)
CRE (mg/dL)	0.7 (0.1)	0.7 (0.1)	0.7 (01)	0.7 (0.1)	0.6 (0.0)	0.7 (0.0)	0.7 (0.1)	0.7 (0.1)	0.66(0.12)
BUN (mg/dL)	23.9 (3.5)	28.1 (4.3)**	25.6 (4.2)*	19.8 (6.1)*	27 (1.0)	30.2 (7.8)*	25.1 (2.4)	19.1 (5.7)	20.5(3.7)
CK (U/L)	147 (66)	128 (32)	69 (23)	214 (93)**	158 (44)	303 (86)**	229 (200)*	553 (4)**	126(50)
D-dimer (μg/ml)	0.7 (0.1)	1.2 (0.3)	0.9 (0.3)	-	1.3 (0.5)	1.3 (0.2)	1.1 (0.1)	-	-
Fibrinogen A (mg/dl)	-	170 (23)	190 (20)	-	-	176 (1.4)	205 (13)	-	-

Values are presented as mean (SD). For each animal, blood was sampled at four time points: 55–104 days (Post-1), 110–180 days (Post-2), 196–217 days (Post-3), and 350–470 days (Post-4) after transplantation. Normal values were obtained from animals 3 years old or younger. -: not obtained. *one or **two animals in the corresponding group had values outside the normal range of values ± 2SD. Although normal D-dimer and fibrinogen A values were not obtained in cynomolgus monkeys, they were close to the normal range of humans (D-dimer: <1.0 mg/ml and fibrinogen A <380 mg/dl).

Please cite this article as: Wakao, S., et al., Long-term observation of auto-cell transplantation in non-human primate reveals safety and efficiency of bone marrow stromal cell-derived Schwann..., Exp. Neurol. (2010), doi:10.1016/j.expneurol.2010.01.022

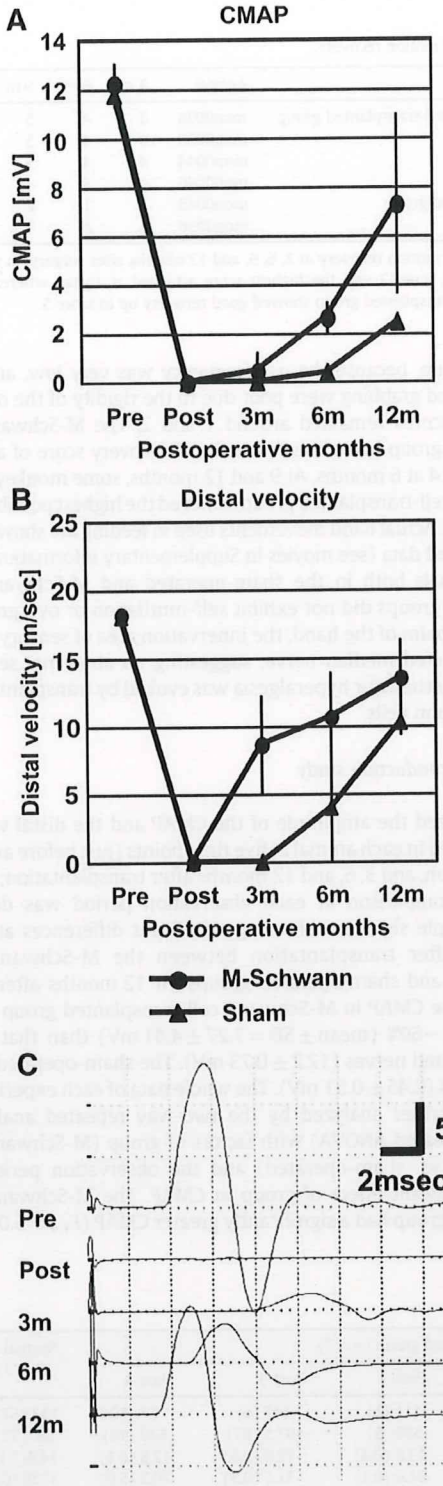

Fig. 4. Results of motor nerve conduction studies. (A) Compound muscle action potential (CMAP, in mV) of the medial nerve, (B) distal velocity (m/s) of the median nerve and (C) the actual wave forms of the CMAP for an example of the M-Schwann cell-transplanted group. Pre; before transplantation, Post; just after transplantation, 3 m, 6 m, and 12 m indicate 3, 6, and 12 months after transplantation, respectively. Values in (A, B) are presented as mean ± SD (mV and m/s, respectively).

tailed $P = 0.04$) than the sham-operated group. These findings suggest that auto-cell transplantation of M-Schwann cells significantly promoted regeneration of the median nerve motor axons distal to the transected site and that this graft contributed about 40% of the grab function at 1 year post-transplantation. In terms of distal velocity, significant promotion was observed at 3 months after transplantation by the two sample sign test, and a significant group effect ($F_{1,4} = 5.85$, one-tailed $P = 0.036$) was demonstrated by the two-way repeated ANOVA, in the M-Schwann cell-transplanted group, but the velocities at 12 months after transplantation were well recovered in both the M-Schwann cell-transplanted group (13.5 ± 4.03 m/s) and the sham-operated group (10.2 ± 1.33 m/s) to a level 60% to 75% of the pre-transplantation (18.0 ± 0.57 m/s) velocity. These findings suggest that saltatory conduction was a little accelerated by the transplanted M-Schwann cells but reached almost a similar level observed in the sham-operated group at 12 months after transplantation because of the contribution of the host Schwann cells in myelin formation and saltatory conduction.

^{18}F-FDG-PET

Although the ^{18}F-FDG-PET test is not completely specific for neoplastic cells, it sensitively detects such cells in most organs. In addition, previous studies revealed that neoplastic transformation of host Schwann cells can be detected by FDG-PET scans (Hamada et al., 2006). Thus, for each animal, we performed ^{18}F-FDG-PET scans to screen for neoplastic transformation of the grafts at 3, 6, and 12 months after transplantation.

We found no abnormal radioactivity accumulation based on standardized uptake value (SUV) images of FDG-PET at any of the three time points (Fig. 5) except in regions of physiologic accumulation and in the vein where the FDG was injected. Importantly, no apparent accumulation was observed at the transplanted site of the animals in any PET scan.

Histological analysis of the graft after 1 year

To estimate the safety of M-Schwann cell transplantation, labeling of cells prior to the transplantation such as lentivirus- or retrovirus-mediated gene introduction of green fluorescent protein or labeling with fluorescent dye was not performed. Therefore, the true ratio of Schwann cell marker expression in transplanted M-Schwann cells could not be evaluated. Furthermore, since host Schwann cells migrate from both proximal and distal nerve segments, host Schwann cells and M-Schwann cells might have intermingled within the grafted tube. For these reasons, we did not attempt to show the grafted cells inside the tube but instead examined the effect of transplanted cells. The effect of Schwann cells in the injured PNS is to promote axonal regeneration and to construct the myelin sheath for saltatory conduction (Fawcett and Keynes, 1990; Hall, 2001; Radtke and Vogt, 2009; Torigoe et al., 1996). Electrophysiological data suggested that transplanted M-Schwann cells contributed to the promotion of axonal regeneration and that myelination level was not significantly different between the M-Schwann cell-transplanted and sham-operated groups. In this regard, we evaluated the effect of transplanted cells by immunohistochemistry for NF to detect the amount of regenerated axons inside the grafted tube (McKay Hart et al., 2002). The immunohistochemistry for NF in the transverse sections of the middle portion of the grafted tube is shown in Fig. 6. Also, the NF-positive axons inside the tube seemed more condensed, particularly at the site just beneath the inner wall of the tube, in the M-Schwann cell-transplanted group compared to the control group (Figs. 6C and D). The ratios of the NF-positive area to the total nerve area in each animal were calculated (see Materials and methods) as 51.5 ± 7.55% and 33.3 ± 1.11% in the M-Schwann cell-transplanted and sham-operated groups, respectively. The ratio of the NF-positive area in the M-Schwann cell-transplanted group was significantly greater than that in the sham-operated group (one-tailed $P<0.05$, Student's t-test with Bonferroni correction). The NF-positive area

Please cite this article as: Wakao, S., et al., Long-term observation of auto-cell transplantation in non-human primate reveals safety and efficiency of bone marrow stromal cell-derived Schwann..., Exp. Neurol. (2010), doi:10.1016/j.expneurol.2010.01.022

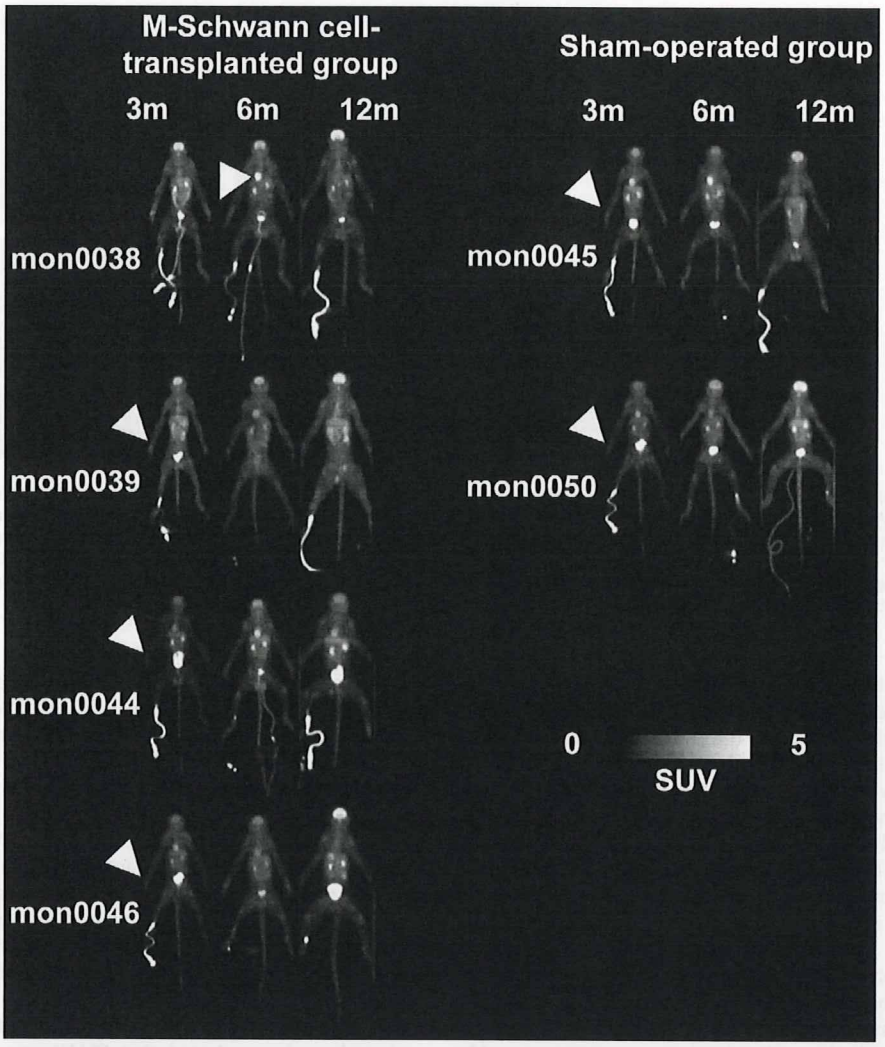

Fig. 5. Results of the whole-body ^{18}F-fluorodeoxyglucose (FDG)-positron emission tomography (PET) performed to screen for neoplastic transformation of the grafted cells. In PET images, the frontal view of the animal is presented by maximal intensity projection. Arrowheads indicate the grafted sites, the distal median nerve (left in mon0038, and right in the other animals). Abnormal accumulation (cut-off = 2.5 in SUV) was not observed in any PET scan except in regions known to have physiologic accumulations of FDG: brain, heart, kidney, urinary tracts, and injection site. SUV: standardized uptake value. 3 m, 6 m, and 12 m indicate 3, 6, and 12 months after graft transplantation.

significantly correlated with the CMAP measurement just before autopsy (measured at 12 months after operation; Pearson's correlation coefficient = 0.81, $P<0.05$). While transplanted M-Schwann cells were not distinguishable from host Schwann cells, double-immunostaining for NF and MAG on transverse sections both of the M-Schwann cell-transplanted and sham-operated groups (Figs. 6E and F, respectively) confirmed myelination of regenerated axons. As was predicted by results of electrophysiology taken at 12 months, the extent of myelination was almost similar in both experimental groups. These data suggest that the improvement observed in behavioral and electrophysiological assessment was provided by transplanted M-Schwann cells in regard to their function in promoting axonal regeneration rather than in facilitation of myelination of regenerated axons.

To observe the immune response against the transplanted graft, immunohistochemistry against CD163, a specific marker for monocytes and macrophages, was performed (Supplementary Fig. 3). Inside the graft, CD163+ cells were scarcely observed at the middle portion of the graft and some cells were found near (<300 μm) by the wall of the graft. Although CD163+ cells were observed inside the graft, the number of CD163+ cells inside the graft in the M-Schwann cell-transplanted group was as small as 1.50 ± 0.41 cells in 0.1 mm^2 and was not significantly different from 1.44 ± 0.51 cells, that in the sham-operated group, indicating that the sustained rejection of transplanted M-Schwann cells was not prominently exerted after transplantation. More CD163+ cells were observed in the wall of the graft both in the sham-operated and M-Schwann cell-transplanted groups, indicating the process of bio-degradation of the grafted tube.

Local tumor formation was evaluated by the detection of proliferating cells with Ki67-immunostaining (Fig. 7), showing no statistically significant difference between Ki67-positive cells inside the grafted tube in the M-Schwann cell-transplanted and sham-operated groups: 2.88 ± 0.67 cells and 3.25 ± 1.00 cells/0.1 mm^2, respectively. Also, these proliferating cells exhibited no mass formation. These findings indicate that transplanted M-Schwann cells did not exhibit local tumor formation.

Discussion

In the present study, we estimated the safety and effectiveness of transplanting M-Schwann cells into non-human primates over a 1-year period. Schwann cells induce neural regeneration and enable

Please cite this article as: Wakao, S., et al., Long-term observation of auto-cell transplantation in non-human primate reveals safety and efficiency of bone marrow stromal cell-derived Schwann..., Exp. Neurol. (2010), doi:10.1016/j.expneurol.2010.01.022

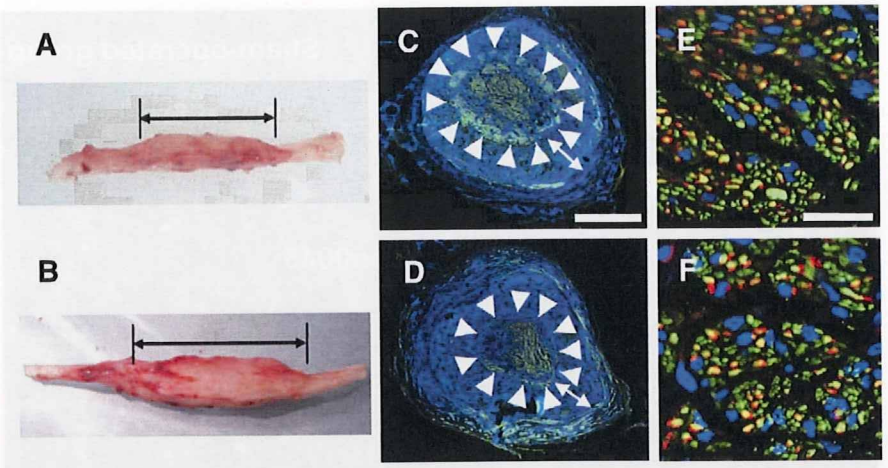

Fig. 6. Grafted monkey median nerves at 12 months. (A, B) Appearance of grafted monkey median nerves. Arrows indicate approximate position of grafts in mon0039 (M-Schwann cell-transplanted group) (A) and mon0045 (sham-operated group) (B). (C–F) Immunohistochemistry of transverse sections in the middle portion of the graft in mon0039 (M-Schwann cell-transplanted group) (C, E) and mon0045 (sham-operated group) (D, F). Immunostaining for neurofilament (NF) (green) exhibited massive axonal regeneration just beneath the inner wall of the tube (arrowheads) in the M-Schwann cell-transplanted group (C), but not in the sham-operated group (D). Arrows in C and D indicate the wall of the grafted tube. Immunofluorescence against NF (green) and myelin-associated glycoprotein (red) showed myelination of regenerated axons (E, F). The extent of myelination of regenerated axons was almost similar in both experimental groups. DAPI (blue) was used for the counterstaining of nuclei. Scale bars: 500 μm (C, D) and 40 μm (E, F).

saltatory conduction by producing myelin, and are expected to be applied to PNS and CNS injuries. In the case of the monkey study, PNS injury models are easily approved by the ethics committee for animal experimentation rather than spinal cord injury. We therefore examined the effectiveness and safety of our system in a monkey median nerve injury model. Cells that expressed Schwann cell markers could be efficiently induced from cynomolgus monkey MSCs, similar to rat and human MSCs (Dezawa et al., 2001, Shimizu et al., 2007). Auto-cell transplantation of M-Schwann cells in monkey median nerve injury model resulted in successful nerve regeneration and functional recovery.

Cell labeling is effective in tracing the fate of transplanted cells and this method is categorized into two techniques such as exogenous gene introduction and staining with a fluorescent dye. Gene introduction by virus infection such as lentivirus or retrovirus enables permanent cell labeling, while this method is also known to evoke a hazardous risk of carcinogenesis (Hacein-Bey-Abina et al., 2003). Fluorescence dyes such as DiI or PKH26 have been used for cell labeling for transplantation study but these dyes also have cytotoxicity and might not exhibit sufficient fluorescence intensity after prolonged period such as 1 year. For these reasons, we did not perform labeling of M-Schwann cells in this study. Based on the lack of any signs of tumor formation in FDG-PET scanning and in immunohistochemistry for proliferation marker for up to 1 year in any of the M-Schwann cell-transplanted animals, and the absence of serious problems in the general health and histological study, our system is very likely to be safe. In our previous report, M-Schwann cells induced from human MSCs were transplanted into a rat model of sciatic nerve transection under immunosuppression, and were shown to contribute to re-myelination of regenerating axons and functional recovery (Shimizu et al., 2007). Also, we previously examined the safety of M-Schwann cells induced from human MSCs transplanted into uninjured nude-mice striatum followed-up for 6 months (unpublished data). Tumor formation was not observed in pathologic analysis and the general health of transplanted nude-mice showed no serious problems. These results together support the idea that human MSC-derived Schwann cells may also be safe and effective for cell-based therapy.

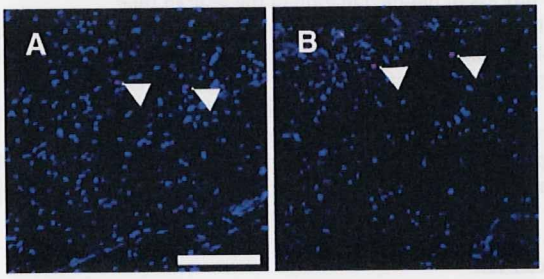

Fig. 7. Immunohistochemistry inside the grafted tube. Small numbers of Ki67-positive cells (red, arrowheads) were found in both the M-Schwann cell-transplanted (A) and also sham-operated (B) groups. DAPI (blue) was used for the counterstaining of nuclei. Scale bar: 100 μm.

Our results indicate that the M-Schwann cells contributed to functional recovery after transplantation in the injured PNS. Electrophysiology demonstrated that CMAP was much improved in the M-Schwann cell-transplanted group compared with the sham-operated group, suggesting regeneration of a larger number of axons promoted by the transplanted M-Schwann cells in this group. This concept was confirmed by histological analysis. The area positive for NF, being considered to be correlated with CMAP, was larger in the M-Schwann cell-transplanted group than in the sham-operated group.

In previous studies, we have demonstrated the myelin formation of M-Schwann cells induced from rat MSCs after transplantation into the injured PNS models even in the ultrastructural level (Dezawa et al., 2001; Ishikawa et al., 2009). In this study, electrophysiological data regarding distal velocity was accelerated in the M-Schwann cell-transplanted group compared with those of the sham-operated group. However, the biodegradable conduit used in this study itself has the property to support regenerating axons (Hisasue et al., 2005). As mentioned in Results, host Schwann cells also join to promote axonal regeneration and to form myelin sheath. This process might be enhanced by the biodegradable conduit used in this study and might mask the function of M-Schwann cells on saltatory conduction at later observation period such as 6 and 12 months after transplantation. Whether the transplanted M-Schwann cells can form myelin sheath to contribute efficient saltatory conduction should be assessed in future studies by labeling cells with either a genetic modification or fluorescent dyes prior to transplantation.

Because the induction system for M-Schwann cells comprises a cell density adjustment at the first step followed by a series of treatments with BME, RA, and a set of cytokines, M-Schwann cells can be induced

Please cite this article as: Wakao, S., et al., Long-term observation of auto-cell transplantation in non-human primate reveals safety and efficiency of bone marrow stromal cell-derived Schwann..., Exp. Neurol. (2010), doi:10.1016/j.expneurol.2010.01.022

by a rather simple and stable process without gene introduction, and thus the system is a realistic source of cell therapy for PNS and CNS regeneration. The induction of cells with Schwann cell properties was recently reported in embryonic stem cells and skin-derived neural crest cells, but their effectiveness and safety in terms of tumor formation and problems that might arise need to be examined because of potential ethical concerns (Roth et al., 2007).

MSCs provide potential possibilities for clinical application, since they can be efficiently expanded in vitro to acquire a therapeutic scale. Different from embryonic stem cells or fetus/embryo-derived cells, MSCs are easily accessible through aspiration of the bone marrow, and can be easily expanded in large scale for auto-transplantation. MSCs can be collected without serious ethical problems, and there is no need to use fertilized eggs or fetuses, which is a great advantage for clinical use. In addition, as MSCs are also obtained from marrow banks, transplantation of induced cells with the same HLA subtype from a healthy donor may minimize the risks of rejection in allo-transplantation.

In the present study, we chose the PNS injury model to show the safety and efficiency of M-Schwann cells, in which M-Schwann cells were induced prior to, and transplanted immediately after, the injury. This model, however, is not a representative of clinical situations. Virtually, it needs more than 1 week to prepare M-Schwann cells after harvesting MSCs. Further studies are necessary for confirming the effectiveness of M-Schwann cells in delayed transplantation in PNS injury.

Our previous studies have demonstrated that Schwann cells induced from MSCs exert trophic effects, provide a strong foothold for regenerating axons, and re-construct myelin to support saltatory conduction (Dezawa et al., 2001; Ishikawa et al., 2009; Kamada et al., 2005; Mimura et al., 2004; Shimizu et al., 2007; Someya et al., 2008). Therefore, induced Schwann cells are a valuable candidate source for cell therapy in peripheral nerve injury, and this study suggests that auto-cell transplantation of M-Schwann cells is also hopeful for application to spinal cord injury.

Acknowledgments

We thank to Dr. J. J. Archelos (Karl-Franzens Universitat, Graz, Austria) for providing us the P0 antibody and to Ms. Mori E., Ms. Kotera J. and Ms. Mamiya R. for their technical assistance. This study was supported by the Program for Promotion of Fundamental Studies in Health Sciences of the National Institute of Biomedical Innovation (NIBIO, 05-6) and by the Health and Labor Sciences Research Grants of "Research on Psychiatric and Neurological Diseases and Mental Health" from the Ministry of Health, Labor and Welfare. The study was also supported by Grant-in-Aid for Scientific Research (B) (19390074) from the Ministry of Education, Culture, Sports, Science and Technology Japan.

Appendix A. Supplementary data

Supplementary data associated with this article can be found, in the online version, at doi:10.1016/j.expneurol.2010.01.022.

References

Ahmed, Z., Brown, R.A., Ljungberg, C., Wiberg, M., Terenghi, G., 1999. Nerve growth factor enhances peripheral nerve regeneration in non-human primates. Scand. J. Plast. Reconstr. Surg. Hand Surg. 33, 393–401.

Al-Sugair, A., Coleman, R.E., 1998. Applications of PET in lung cancer. Semin. Nucl. Med. 28, 303–319.

Archibald, S.J., Shefner, J., Krarup, C., Madison, R.D., 1995. Monkey median nerve repaired by nerve graft or collagen nerve guide tube. J. Neurosci. 15, 4109–4123.

Auba, C., Hontanilla, B., Arcocha, J., Gorria, O., 2006. Peripheral nerve regeneration through allografts compared with autografts in FK506-treated monkeys. J. Neurosurg. 105, 602–609.

Bunge, M.B., 2002. Bridging the transected or contused adult rat spinal cord with Schwann cell and olfactory ensheathing glia transplants. Prog. Brain Res. 137, 275–282.

Bunge, M.B., 2008. Novel combination strategies to repair the injured mammalian spinal cord. J. Spinal Cord Med. 31, 262–269.

Dezawa, M., Adachi-Usami, E., 2000. Role of Schwann cells in retinal ganglion cell axon regeneration. Prog. Retin. Eye Res. 19, 171–204.

Dezawa, M., Takahashi, I., Esaki, M., Takano, M., Sawada, H., 2001. Sciatic nerve regeneration in rats induced by transplantation of in vitro differentiated bone-marrow stromal cells. Eur. J. NeuroSci. 14, 1771–1776.

Fawcett, J.W., Keynes, R.J., 1990. Peripheral nerve regeneration. Annu. Rev. Neurosci. 13, 43–60.

Hacein-Bey-Abina, S., Von Kalle, C., Schmidt, M., McCormack, M.P., Wulffraat, N., Leboulch, P., Lim, A., Osborne, C.S., Pawliuk, R., Morillon, E., Sorensen, R., Forster, A., Fraser, P., Cohen, J.I., de Saint Basile, G., Alexander, I., Wintergerst, U., Frebourg, T., Aurias, A., Stoppa-Lyonnet, D., Romana, S., Radford-Weiss, I., Gross, F., Valensi, F., Delabesse, E., Macintyre, E., Sigaux, F., Soulier, J., Leiva, L.E., Wissler, M., Prinz, C., Rabbitts, T.H., Le Deist, F., Fischer, A., Cavazzana-Calvo, M., 2003. LMO2-associated clonal T cell proliferation in two patients after gene therapy for SCID-X1. Science 302, 415–419.

Hall, S., 2001. Nerve repair: a neurobiologist's view. J. Hand Surg. [Br] 26, 129–136.

Hamacher, K., Coenen, H.H., Stocklin, G., 1986. Efficient stereospecific synthesis of no-carrier-added 2-[18F]-fluoro-2-deoxy-D-glucose using aminopolyether supported nucleophilic substitution. J. Nucl. Med. 27, 235–238.

Hamada, K., Tomita, Y., Ueda, T., Enomoto, K., Kakunaga, S., Myoui, A., Higuchi, I., Yoshikawa, H., Hatazawa, J., 2006. Evaluation of delayed 18F-FDG PET in differential diagnosis for malignant soft-tissue tumors. Ann. Nucl. Med. 20, 671–675.

Hess, J.R., Brenner, M.J., Fox, I.K., Nichols, C.M., Myckatyn, T.M., Hunter, D.A., Rickman, S.R., Mackinnon, S.E., 2007. Use of cold-preserved allografts seeded with autologous Schwann cells in the treatment of a long-gap peripheral nerve injury. Plast. Reconstr. Surg. 119, 246–259.

Hill, C.E., Moon, L.D., Wood, P.M., Bunge, M.B., 2006. Labeled Schwann cell transplantation: cell loss, host Schwann cell replacement, and strategies to enhance survival. Glia 53, 338–343.

Hisasue, S., Kato, R., Sato, Y., Suetomi, T., Tabata, Y., Tsukamoto, T., 2005. Cavernous nerve reconstruction with a biodegradable conduit graft and collagen sponge in the rat. J. Urol. 173, 286–291.

Ishikawa, N., Suzuki, Y., Dezawa, M., Kataoka, K., Ohta, M., Cho, H., Ide, C., 2009. Peripheral nerve regeneration by transplantation of BMSC-derived Schwann cells as chitosan gel sponge scaffolds. J. Biomed. Mater. Res. A 89, 1118–1124.

Jiang, L., Zhu, J.K., Liu, X.L., Xiang, P., Hu, J., Yu, W.H., 2008. Differentiation of rat adipose tissue-derived stem cells into Schwann-like cells in vitro. NeuroReport 19, 1015–1019.

Kamada, T., Koda, M., Dezawa, M., Yoshinaga, K., Hashimoto, M., Koshizuka, S., Nishio, Y., Moriya, H., Yamazaki, M., 2005. Transplantation of bone marrow stromal cell-derived Schwann cells promotes axonal regeneration and functional recovery after complete transection of adult rat spinal cord. J. Neuropathol. Exp. Neurol. 64, 37–45.

Kingham, P.J., Kalbermatten, D.F., Mahay, D., Armstrong, S.J., Wiberg, M., Terenghi, G., 2007. Adipose-derived stem cells differentiate into a Schwann cell phenotype and promote neurite outgrowth in vitro. Exp. Neurol. 207, 267–274.

Kitada, M., Chakrabortty, S., Matsumoto, N., Taketomi, M., Ide, C., 2001. Differentiation of choroid plexus ependymal cells into astrocytes after grafting into the pre-lesioned spinal cord in mice. Glia 36, 364–374.

Kitada, M., Rowitch, D.H., 2006. Transcription factor co-expression patterns indicate heterogeneity of oligodendroglial subpopulations in adult spinal cord. Glia 54, 35–46.

Lee, S.J., Lim, A.Y., Lim, I.J., Lim, T.C., Pho, R.W., 2008. Innervation of the face studied using modifications to Sihler's technique in a primate model. Plast. Reconstr. Surg. 121, 1188–1205.

McKay Hart, A., Brannstrom, T., Wiberg, M., Terenghi, G., 2002. Primary sensory neurons and satellite cells after peripheral axotomy in the adult rat: timecourse of cell death and elimination. Exp. Brain Res. 142, 308–318.

Mimura, T., Dezawa, M., Kanno, H., Sawada, H., Yamamoto, I., 2004. Peripheral nerve regeneration by transplantation of bone marrow stromal cell-derived Schwann cells in adult rats. J. Neurosurg. 101, 806–812.

Mligiliche, N.L., Tabata, Y., Kitada, M., Endoh, K., Okamato, K., Fujimoto, E., Ide, C., 2003. Poly lactic acid–caprolactone copolymer tube with a denatured skeletal muscle segment inside as a guide for peripheral nerve regeneration: a morphological and electrophysiological evaluation of the regenerated nerves. Anat. Sci. Int. 78, 156–161.

Nagane, K., Kitada, M., Wakao, S., Dezawa, M., Tabata, Y., 2009. Practical induction system for dopamine-producing cells from bone marrow stromal cells using spermine-pullulan-mediated reverse transfection method. Tissue Eng. Part A 15, 1655–1665.

Pittenger, M.F., Mackay, A.M., Beck, S.C., Jaiswal, R.K., Douglas, R., Mosca, J.D., Moorman, M.A., Simonetti, D.W., Craig, S., Marshak, D.R., 1999. Multilineage potential of adult human mesenchymal stem cells. Science 284, 143–147.

Plant, G.W., Chirila, T.V., Harvey, A.R., 1998. Implantation of collagen IV/poly(2-hydroxyethyl methacrylate) hydrogels containing Schwann cells into the lesioned rat optic tract. Cell Transplant. 7, 381–391.

Prockop, D.J., 1997. Marrow stromal cells as stem cells for nonhematopoietic tissues. Science 276, 71–74.

Radtke, C., Vogt, P.M., 2009. Peripheral nerve regeneration: a current perspective. Eplasty 9, e47.

Roth, T.M., Ramamurthy, P., Ebisu, F., Lisak, R.P., Bealmear, B.M., Barald, K.F., 2007. A mouse embryonic stem cell model of Schwann cell differentiation for studies of the role of neurofibromatosis type 1 in Schwann cell development and tumor formation. Glia 55, 1123–1133.

Shimizu, S., Kitada, M., Ishikawa, H., Itokazu, Y., Wakao, S., Dezawa, M., 2007. Peripheral nerve regeneration by the in vitro differentiated-human bone marrow stromal cells with Schwann cell property. Biochem. Biophys. Res. Commun. 359, 915–920.

Please cite this article as: Wakao, S., et al., Long-term observation of auto-cell transplantation in non-human primate reveals safety and efficiency of bone marrow stromal cell-derived Schwann..., Exp. Neurol. (2010), doi:10.1016/j.expneurol.2010.01.022

Someya, Y., Koda, M., Dezawa, M., Kadota, T., Hashimoto, M., Kamada, T., Nishio, Y., Kadota, R., Mannoji, C., Miyashita, T., Okawa, A., Yoshinaga, K., Yamazaki, M., 2008. Reduction of cystic cavity, promotion of axonal regeneration and sparing, and functional recovery with transplanted bone marrow stromal cell-derived Schwann cells after contusion injury to the adult rat spinal cord. J. Neurosurg. Spine 9, 600–610.

Torigoe, K., Tanaka, H.F., Takahashi, A., Awaya, A., Hashimoto, K., 1996. Basic behavior of migratory Schwann cells in peripheral nerve regeneration. Exp. Neurol. 137, 301–308.

Vukovic, J., Plant, G.W., Ruitenberg, M.J., Harvey, A.R., 2007. Influence of adult Schwann cells and olfactory ensheathing glia on axontarget cell interactions in the CNS a comparative analysis using a retinotectal cograft model. Neuron Glia Biol. 3, 105–117.

Xu, Y., Liu, Z., Liu, L., Zhao, C., Xiong, F., Zhou, C., Li, Y., Shan, Y., Peng, F., Zhang, C., 2008. Neurospheres from rat adipose-derived stem cells could be induced into functional Schwann cell-like cells in vitro. BMC Neurosci. 9, 21.

Please cite this article as: Wakao, S., et al., Long-term observation of auto-cell transplantation in non-human primate reveals safety and efficiency of bone marrow stromal cell-derived Schwann..., Exp. Neurol. (2010), doi:10.1016/j.expneurol.2010.01.022

V. 治　　療

再生療法

骨髄間葉系細胞を用いた自己細胞移植の可能性

Auto-cell transplantation for Parkinson's disease; induction of dopaminergic neurons from bone marrow stromal cells

林　拓也[1]　　出澤真理[2]

Key words：間葉系細胞，骨髄，分化転換，幹細胞，パーキンソン病

はじめに

骨髄には造血系細胞とは別に骨髄間葉系細胞(bone marrow stromal cells: MSC)という細胞があり，骨髄穿刺で採取した骨髄液を培養することにより接着性細胞として容易に得ることができる．増殖力が非常に旺盛で，短期間で移植にもっていけるだけの細胞数を確保することが可能である．例えば数10-100ccの骨髄液を培養すれば数週間で約1,000万個の細胞を確保できるうえに，患者本人の細胞を利用すれば，死亡胎児や受精卵を使う必要がなく，免疫拒絶の問題も回避できる．MSCは現実的な利点の多い細胞である．

MSCは同じ間葉系に属する骨，軟骨，脂肪に分化することは以前より知られているが，最近培養条件下で様々な因子を投与することにより胚葉を超えた分化転換が報告され，この細胞のもつ利点も併せて注目が集まってきている[1-3]．また，多くの種類のサイトカインを産生するというこの細胞のもつ特性から脊髄損傷や脳梗塞などの神経系疾患における組織の救済・温存に利用する試みもある[4-6]．

このように様々な可能性をもつ細胞であるが，著者らはヒトMSCから脊髄損傷などの神経再生能を有する末梢性グリアであるSchwann細胞，神経細胞，骨格筋細胞を高い効率で誘導する方法を確立し，神経・筋変性疾患への応用に向けて研究を展開している．

本稿ではドーパミン産生細胞の誘導とパーキンソン病への応用の可能性を考察したいと思う．

パーキンソン病の細胞移植治療は，1980年代後半から胎児中絶脳のドーパミン細胞移植術が行われたものの倫理面や免疫拒絶反応の点から一般には行われていない．その後，自己の副腎髄質細胞や交感神経節細胞の移植なども試験されるも有効性は確立せず，近年のES細胞の発見を契機に再度注目を浴びている．パーキンソン病はプラセボ効果の生じやすい疾患として知られ，特に外科治療を開発する際には有効性を客観的・多面的に示すことが重要である．著者らは齧歯類だけでなく高等哺乳類(霊長類動物)のパーキンソン病モデルで前臨床試験を行い，ポジトロンエミッショントモグラフィ(PET)を用いて非侵襲的にドーパミン機能を評価することで自己骨髄間質細胞由来のDA細胞移植術の有効性・安全性試験を進めておりその一部も概説する．

[1]Takuya Hayashi: Department of Investigative Radiology, Advanced Medical Engineering Center, National Cardiovascular Center Research Institute　国立循環器病センター研究所 先進医工学センター 放射線医学部　[2]Mari Dezawa: Department of Stem Cell Biology and Histology, Tohoku University Graduate School of Medicine　東北大学大学院医学系研究科 細胞組織学分野

0047-1852/09/¥40/頁/JCLS

1. 神経細胞の誘導

Notch遺伝子は発生・分化を制御することで知られており，幹細胞の維持，神経や骨格筋の分化制御など多くの機能をもつ[7]．神経発生においてはグリア誘導因子として作用するが，MSCにNotchを作用させると神経細胞への分化が誘導される[8]．MSCのNotchに対する特異な反応は後で触れるが，MSCは患者本人から大量に採れるので，この現象を検討すれば，自己由来の神経細胞を大量に得ることにつながる方法になるのではと考えて検証を進め，神経誘導システムを確立した．

constitutive active formのNotch1細胞内ドメイン(Notch intracellular domain: NICD)遺伝子をpCI-neoプラスミドに組み込みlipofectionで導入し選択すると，MSCは神経前駆細胞のマーカーであるnestin，NeuroD，Sox2などを発現し，promoter解析においてもこれらの活性上昇が認められる[2]．更に神経幹細胞の培地で浮遊培養するとneurosphereが多数形成される．これらのneurosphereを分化培地に移すことにより，ほとんどの細胞がTuj-1，MAP2陽性の神経細胞に分化することから，グリア細胞というよりむしろ神経細胞に特化した前駆細胞が得られたと考えられる[8]．

MSCにNotchを導入した上記の細胞を特定の細胞密度にまき直し，血清存在下で線維芽細胞増殖因子(bFGF)，細胞内cAMP上昇作用をもつフォルスコリン(forskloin)と毛様体神経栄養因子(CNTF)の3種を同時に投与することによって非常に高い効率(96％前後)で神経細胞誘導が引き起こされる[8]．誘導された神経細胞はBrd-U取り込み実験からpost-mitotic neuronであることが確認され，更にパッチクランプ実験において活動電位を認めたことから機能的な神経細胞であると考えられる．またこの操作の一つ前のsphereを用いた実験でも確認されたように，この細胞群にはグリア細胞が含まれていないという特徴をもっている[8]．

2. MSCにおけるNotchと神経誘導

神経発生においてNotchは神経分化を抑制しグリア分化を促進する因子として知られているが[7]，本システムではMSCにNICDを導入することで選択的に神経細胞が誘導されており，これまで知られている発生学でのNotchの作用からすれば，逆の作用をもたらしたように見受けられる．ただし念頭に置かなくてはならないのは，この現象は発生過程にある神経幹細胞ではなく，成体の骨髄から培養されてきた間葉系の細胞で起きた現象であるということである．この違いはNotch刺激を受け取る細胞内環境の違いによっていると推定され，また，同じNotchのシグナルを受け取っても，結果として観察される現象が異なることはありうる．

RT-PCRを用いて誘導過程における関連因子の発現を調べたところ，誘導前の無処理の状態においてneurogenic因子(Math1，Mash1，Neurogenin)とgliogenic因子(STAT1，STAT3，Hes1，Hes5)の両方の発現が認められるが，NICDの導入によってSTAT1，STAT3の発現抑制が，次いでサイトカイン刺激による神経誘導においてHes1，Hes5の発現抑制がみられ，最終的な神経細胞群においてはneurogenic因子の発現のみが残る[8]．このことが，本システムにおいて神経細胞だけが誘導され，グリア細胞が誘導されてこなかった説明の一つと考えている[8]．

Notchは膜貫通型の膜タンパクであり，リガンドのDelta/Jaggedが結合するとプロテアーゼで細胞膜ドメインが切断され，核内に移行し転写複合体を形成してエフェクターHes1，Hes5を誘導する[7]．これがいわゆるNotchシグナル系であるが，本誘導システムではNICDの導入によるHes1，Hes5の誘導は認められず，NICDの作用をHesで置換することもできなかったことから，MSCには発生過程の細胞とは異なる特有のシステムが存在すると思われる．2006年にAG. Smithらは，Notchの細胞質ドメインをESに導入すると神経幹細胞様に分化し，更にそこから神経細胞のみが自発的に分化した

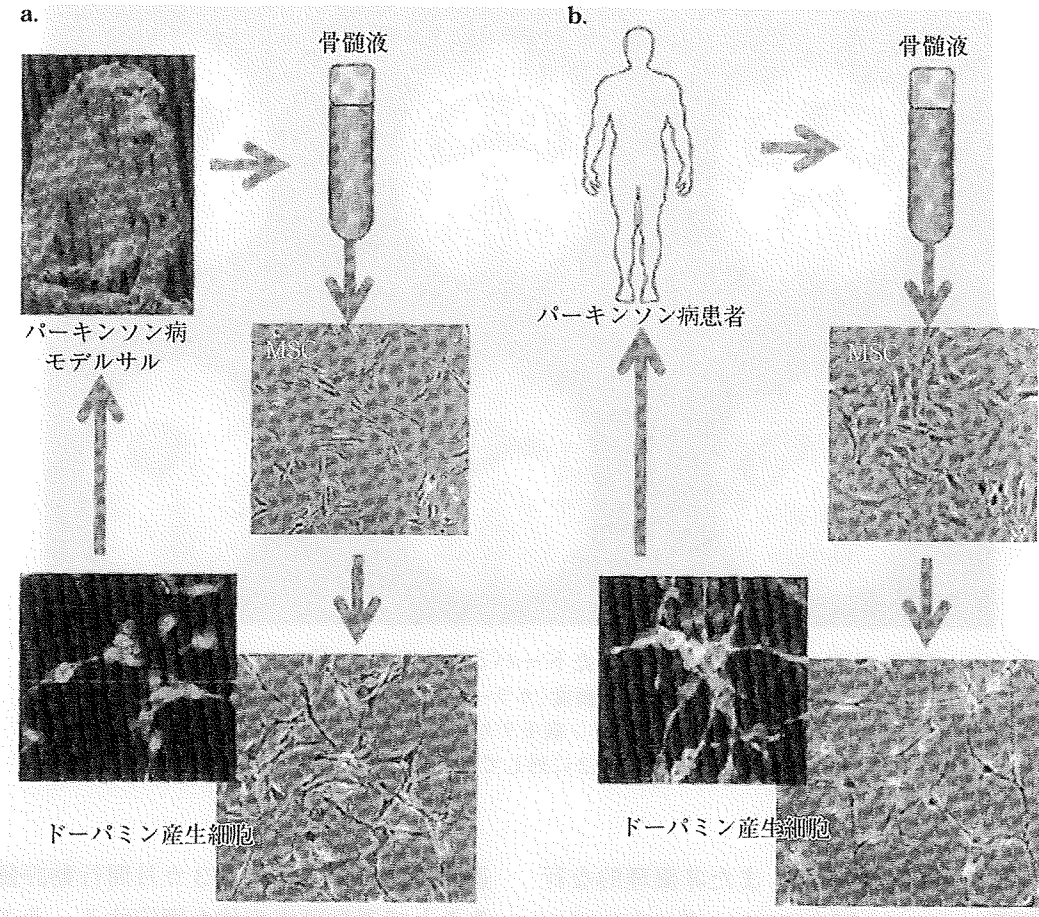

図1 MSCからのドーパミン産生細胞の誘導と自己細胞移植

a: カニクイザル片側性パーキンソン病モデルにおけるMSC由来ドーパミン産生細胞の自己細胞移植の概要．サルなどの高等哺乳類での安全性，有効性の検証が臨床応用における前提となる．
b: パーキンソン病患者におけるMSCを用いたドーパミン産生細胞の自己細胞移植の概要．

と報告しており，この現象はMSCにおける本システムと何らかの共通機構を示唆するものとして非常に興味深い[9]．

3. 神経変性モデル動物への移植

誘導した神経細胞は，前述のようにpost-mitotic neuronであり，形態的にも機能的にも神経細胞の特性を有しているが，特定の神経伝達物質を産生しているものは少ない．神経伝達物質ないしその関連タンパクに対する免疫反応はどれも数パーセント以内であり，特にドーパミンニューロンのマーカーであるTHは3-4％前後であった[8]．

パーキンソン病モデルへの応用においてはドーパミン産生細胞の移植が有効である．そこで中脳ドーパミン神経の発生を促進することで知られているglial-cell line derived neurotrophic factor(GDNF)をヒトおよびラットMSCから誘導した神経細胞に投与したところ，TH陽性率が30-40％に上昇し，培養上清中のK^+濃度上昇による脱分極で～1.1pM/10^6 cellsドーパミンが放出されることを高性能液体クロマトグラフィ(HPLC)において確認した(**図1-b**)．これらの誘導されたドーパミン産生細胞が実際に生体において機能するのかを検証するために，6-OHDAによるパーキンソン病モデルラットを作成し，線条体に約10万個のラット由来の細胞を移植したところ，移植側における脳内でのドーパミン産生能の上昇がHPLCで確認され，またアポモルフィン誘導による異常回転運動の顕著な改善を認めた．免疫抑制剤投与下でヒトMSCから誘導したドーパミン産生細胞を移植

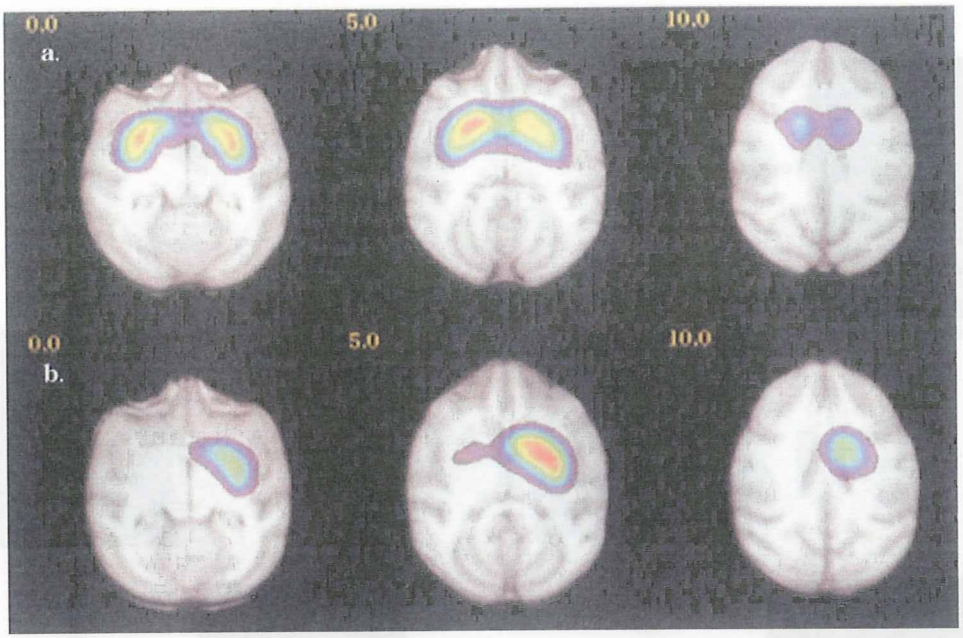

図2 ^{11}C-CFT PETで評価したドーパミントランスポータ（DAT）結合能
a：正常カニクイザルにおける結合能画像（カラー）をMRI-T1画像（白黒）に重ねたもの．b：右側MPTP注入による片側パーキンソン病モデルにおける結合能画像（向かって左側が個体の右側に相当する）．結合能は正常側1.2に対して病側では0.1-0.2程度まで低下している．

しても同様の効果を認めた．また非薬理的な行動機能評価paw-reaching test，adjusting step testにおいても改善が認められた．移植された細胞は脳内においてそのほとんどが神経細胞として生着し，TH，dopamine transporter陽性を示したが，グリア細胞のマーカーを発現するものはなかった[8]．これらのことからMSCから誘導した神経細胞は神経変性モデルにおいて生着し機能回復に寄与することが示唆された[8]．

4. 高等哺乳類におけるパーキンソン病モデル作成と細胞生着・機能発現評価

高等哺乳動物としてカニクイザルを用いた．パーキンソン病モデルはBankiewiczらの方法に従い[10]，右内径動脈よりN-methyl-4-phenyl-1,2,3,6-tetrahydropyridine（MPTP）を注入することで片側性パーキンソン病モデルを作成した．麻酔したサルに血管撮影装置と脳血管カテーテルを使用して右内頸動脈から約20分かけて持続的にMPTP溶液を注入すると約80％の個体で同側の瞳孔が散大する．瞳孔散大した個体は左上肢の不使用・運動寡動などの症状を1週間以内に呈しその後3カ月間行動評価を続けることで運動障害症状も固定する．その段階でパーキンソン病モデルとして細胞移植治療試験に用いた．この時期に，残存するドーパミン機能評価をPETを用いて行うことで定量的に細胞死を評価した．ドーパミン神経細胞が膜表面に発現しているドーパミントランスポータ（DAT）に選択的に結合するリガンド（^{11}C-CFT）を用い脳内のリガンド結合能を評価した．その結果，正常線条体では結合能が1.5程度であるのに対し，MPTP注入側の線条体では0.1程度と極端に結合能が低下していた（**図2**）．対してDA受容体（D1やD2受容体）のリガンドを用いてPETを撮像すると結合能は全く正常に保たれており，これらの所見はヒトのパーキンソン病と酷似した結果が得られた．またDAT結合能の低下度は，サル個体ごとに評価した左上肢運動機能とも良く相関した．一方，移植する骨髄間質細胞由来ドーパミン神経細胞も本来のDA細胞と同様にDATの発現も免疫染色にて確認しえたので，今後この細胞の移植後の生着・機能発現の変化を^{11}C-CFT PETと上肢運動機

能の経時的評価で行い，更に最終的には病理学的，生化学的観察を併せることで有効性・安全性に関する詳細な観察ができると考えられる．

5. パーキンソン病モデルサルの作成と誘導ドーパミン産生細胞の自己細胞移植治療

カニクイザルのMSCは，増殖力は優れているもののlipofectionなどの操作によって細胞障害が大きく，ヒトやラットのMSCと同じ操作によって誘導することが困難である．一方でNICDの導入は神経誘導において必須である．そこでlipofectionではなく，田畑らが開発したreverse transfection法を用いることによってサルMSCへのNICDの導入を行い，導入効率が高くしかも細胞障害が少なくドーパミン産生細胞を得ることができた[11]．この方法で誘導したサルMSCから誘導したドーパミン産生細胞を片側性パーキンソン病モデルサルに自己細胞移植を行っている(**図1-a**)．実際の移植には，サル頭部を脳定位固定装置に固定し高解像度磁気共鳴画像(MRI)を撮像したのちに，その画像を用いて移植部位(MPTP注入側被殻背側後部)を同定し，定位固定装置に装着した注入装置により複数の部位に分けて細胞を注入している．MSC由来ドーパミン産生細胞の自己細胞移植を受けたサルでは^{11}C-CFT PETによってDAT結合能上昇が移植側で認められている．

おわりに

MSCには広く様々な細胞に分化するポテンシャルがある．しかし重要なことは，生体内において仮に自発的に分化転換を起こすとしてもその効率は極めて低く，細胞移植治療に活用できるものではないということである．分化転換によって目的とする細胞を一定量以上得るためには，順序立てた分化誘導操作を行う必要がある．

MSCは骨髄移植の際に既に移植されている細胞であり，旺盛な増殖力をもっている．患者本人や家族からの採取も可能であり，既存の骨髄バンクの登録者から提供を受ける方法もある．特に患者本人の細胞を用いた場合には，免疫拒絶のない自分の細胞を用いた理想的な細胞移植治療，すなわち'自己細胞移植治療'が可能となる(**図1-b**)．しかし実際に治療に応用するためには，安全性，有効性など解決しなければならない多くの課題が残されている．特にNotchの遺伝子導入が操作段階に入っていること，また本来の間葉系細胞から大きく性質を転換させた細胞を移植するとなれば，腫瘍形成の有無を大型哺乳類において検証しなくてはならない．安全面という観点からすれば遺伝子導入ではなくタンパク導入などの方法を用いることによって汎用性が広がると思われる．また安全性・有効性の実際の評価にヒトに近い種である霊長類動物を用いた前臨床試験での詳細な観察と経験が重要で，今後その結果が期待される．

謝辞 本研究は保健医療分野における基礎研究推進事業(05-6)による研究助成を受けて推進したものである．細胞分化培養にかかわった若尾昌平氏(東北大)，カニクイザル実験に携わった寺本 昇，合瀬恭幸，福田肇各氏(国循)，パーキンソン病モデルの作成にかかわった池田博信，伊藤昭人両氏(日精バイリス社，滋賀)に謝意を表する．なお霊長類の試験は国立循環器病センター実験動物委員会の承認を経て行った．

■文　献

1) Pittenger MF, et al: Multilineage potential of adult human mesenchymal stem cells. Science **284**: 143-147, 1999.
2) Mezey E, et al: Turning blood into brain: cells bearing neuronal antigens generated in vivo from bone marrow. Science **290**: 1779-1782, 2000.
3) Makino S, et al: Cardiomyocytes can be generated from marrow stromal cells in vitro. J Clin Invest **103**: 697-705, 1999.
4) Chen J, et al: Therapeutic benefit of intracerebral transplantation of bone marrow stromal cells after cerebral ischemia in rats. J Neurol Sci **189**: 49-57, 2001.